

We will now begin to consider the Universe as a whole. Individual objects such as galaxies and stars will no longer be the subject of discussion, but instead we will turn our attention to the space and time in which these objects are embedded. These considerations will then lead to a world model, the model of our cosmos. We need such a model also to interpret the observations of distant objects, i.e., those with a redshift for which the local Hubble law (1.2) ceases to be valid.

This chapter will deal with aspects of homogeneous cosmology. As we will see, the Universe can, to first approximation, be considered as being homogeneous. At first sight this fact obviously seems to contradict observations because the world around us is highly inhomogeneous and structured. Thus the assumption of homogeneity is certainly not valid on small scales. But observations are compatible with the assumption that the Universe is homogeneous when averaged over large spatial scales. Aspects of inhomogeneous cosmology, and thus the formation and evolution of structures in the Universe, will be considered later in Chap. 7.

4.1 Introduction and fundamental observations

Cosmology is a very special science indeed. To be able to appreciate its peculiar role we should recall the typical way of establishing knowledge in natural sciences. It normally starts with the observation of some regular patterns, for instance the observation that the height h a stone falls through is related quadratically to the time t it takes to fall, $h = (g/2)t^2$. This relation is then also found for other objects and observed at different places on Earth. Therefore, this relation is formulated as the ‘law’ of free fall. The constant of proportionality $g/2$ in this law is always the same. This law of physics is tested by its prediction of how an object falls, and wherever this prediction is tested it is confirmed—disregarding the resistance of air in this simple example, of course.

Relations become physical laws if the predictions they make are confirmed again and again; the validity of such a law is considered more secure the more diverse the tests have been. The law of free fall was tested only on the surface of the Earth and it is only valid there with this constant of proportionality.¹ In contrast to this, Newton’s law of gravity contains the law of free fall as a special case, but it also describes the free fall on the surface of the Moon, and the motion of planets around the Sun. If only a single stone was available, we would not know whether the law of free fall is a property of this particular stone or whether it is valid more generally.

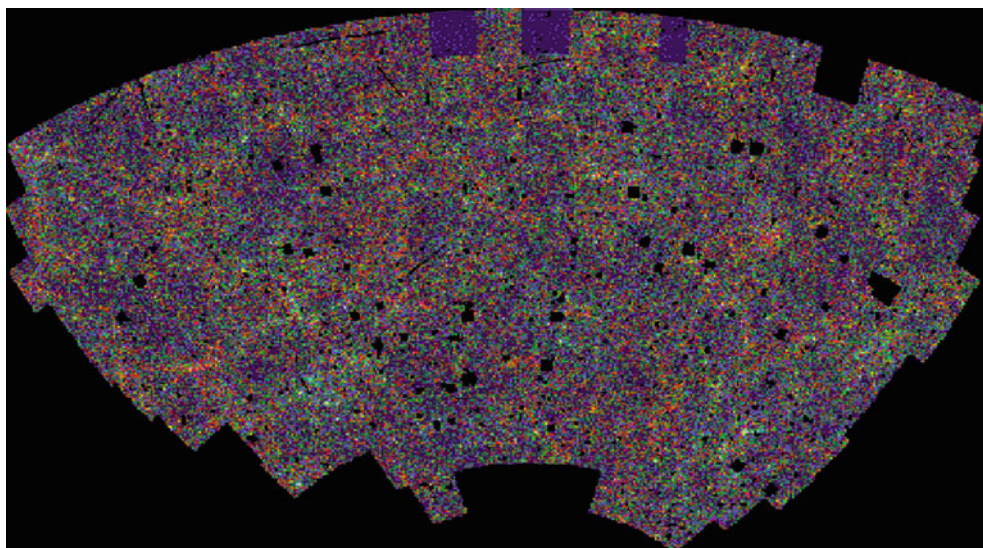
In some ways, cosmology corresponds to the latter example: we have only one single Universe available for observation. Relations that are found in our cosmos cannot be verified in other universes. Thus it is not possible to consider any property of our Universe as ‘typical’—we have no statistics on which we could base a statement like this. Despite this special situation, enormous progress has been made in understanding our Universe, as we will describe here and in subsequent chapters.

Cosmological observations are difficult in general, simply because the majority of the Universe (and with it most of the sources it contains) is very far away from us. Distant sources are very dim. This explains why our knowledge of the Universe runs in parallel with the development of large telescopes and sensitive detectors. Much of today’s knowledge of the distant Universe became available only with the new generation of optical telescopes of the 8-m class, as well as new and powerful telescopes in other wavelength regimes.

The most important aspect of cosmological observations is the finite speed of light. We observe a source at distance D in an evolutionary state at which it was $\Delta t = (D/c)$ younger than today. Thus we can observe the current state of the Universe only very locally. Another consequence of this effect, however, is of even greater importance: due to the finite speed of light, it is possible to look back into the past.

¹Strictly speaking, the constant of proportionality g depends slightly on the location.

Fig. 4.1 The APM-survey: galaxy distribution in a $\sim 100 \times 50$ degree² field around the South Galactic Pole. The intensities of the pixels are scaled with the number of galaxies per pixel, i.e., the projected galaxy number density on the sphere. The ‘holes’ are regions around bright stars, globular clusters etc., that were not surveyed. Credit: S. Maddox, W. Sutherland, G. Efsthathiou & J. Loveday, with follow-up by G. Dalton, and Astrophysics Dept., Oxford University



At a distance of ten billion light years we observe galaxies in an evolutionary state when the Universe had only a third of its current age. Although we cannot observe the past of our own Milky Way, we can study that of other galaxies. If we are able to identify among them the ones that will form objects similar to our Galaxy in the course of cosmic evolution, we will be able to learn a great deal about the typical evolutionary history of such spirals.

The finite speed of light in a Euclidean space, in which we are located at the origin $\mathbf{r} = 0$ today ($t = t_0$), implies that we can only observe points in spacetime for which $|\mathbf{r}| = c(t_0 - t)$; an arbitrary point (\mathbf{r}, t) in spacetime is not observable. The set of points in spacetime which satisfy the relation $|\mathbf{r}| = c(t_0 - t)$ is called our *backward light cone*.

The fact that our astronomical observations are restricted to sources which are located on our backward light cone implies that our possibilities to observe the Universe are fundamentally limited. If somewhere in spacetime there would be a highly unusual event, we will not be able to observe it unless it happens to lie on our backward light cone. Only if the Universe has an essentially ‘simple’ structure will we be able to understand it, by combining astronomical observations with theoretical modeling. Luckily, our Universe seems to be basically simple in this sense.

4.1.1 Fundamental cosmological observations

We will begin with a short list of key observations that have proven to be of particular importance for cosmology. Using these observational facts we will then be able to draw a number of immediate conclusions; other observations will be explained later in the context of a cosmological model.

1. The sky is dark at night (Olbers’ paradox).
2. Averaged over large angular scales, faint galaxies (e.g., those with $R > 20$) are uniformly distributed on the sky (see Fig. 4.1).
3. With the exception of a very few very nearby galaxies (e.g., Andromeda = M31), a redshift is observed in the spectra of galaxies—most galaxies are moving away from us, and their escape velocity increases linearly with distance (Hubble law; see Fig. 1.13).
4. In nearly all cosmic objects (e.g., gas nebulae, main sequence stars), the mass fraction of helium is 25–30%.
5. The oldest star clusters in our Galaxy have an age of ~ 12 Gyr = 12×10^9 yr (see Fig. 4.2).
6. A microwave radiation (cosmic microwave background radiation, CMB) is observed, reaching us from all directions. This radiation is isotropic except for very small, but immensely important, fluctuations with relative amplitude $\sim 10^{-5}$ (see Fig. 1.21).
7. The spectrum of the CMB corresponds, within the very small error bars that were obtained by the measurements with COBE, to that of a perfect blackbody, i.e., a Planck radiation of a temperature of $T_0 = 2.728 \pm 0.004$ K—see Fig. 4.3.
8. The number counts of radio sources at high Galactic latitude does *not* follow the simple law $N(> S) \propto S^{-3/2}$ (see Fig. 4.4).

4.1.2 Simple conclusions

We will next draw a number of simple conclusions from the observational facts listed above. These will then serve as a motivation and guideline for developing the cosmological model. We will start with the assumption of an infinite,

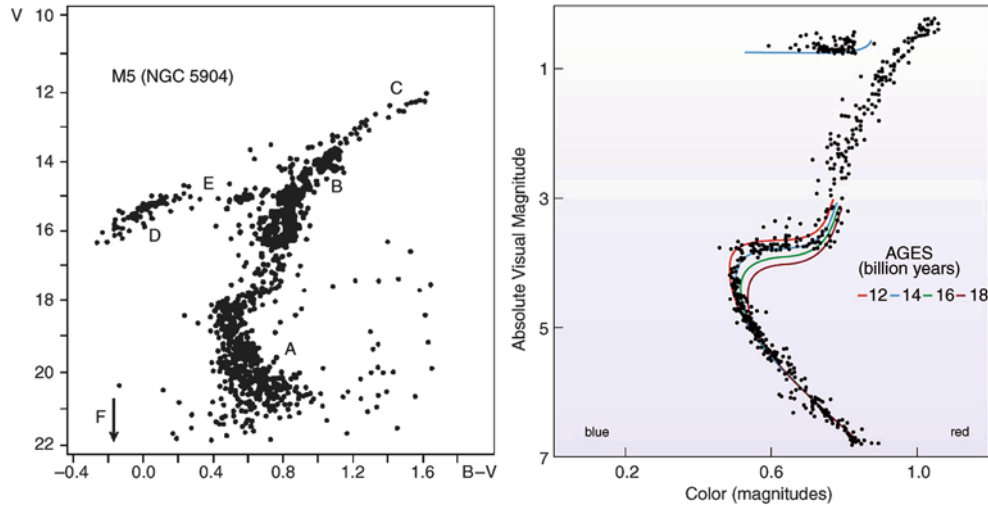


Fig. 4.2 *Left panel:* Color-magnitude diagram of the globular cluster M5. The different sections in this diagram are labeled: A: main sequence; B: red giant branch; C: point of helium flash; D: horizontal branch; E: Schwarzschild-gap in the horizontal branch; F: white dwarfs, below the arrow. At the point where the main sequence turns over to the red giant branch (called the ‘turn-off point’), stars have a mass corresponding to a main-sequence lifetime which is equal to the age of the globular cluster (see Appendix B.3). Therefore, the age of the cluster can be determined from the position of the turn-off point by comparing it with models of stellar evolution. *Right panel:* Isochrones, i.e., curves connecting the stellar evolutionary position in the color-

magnitude diagram of stars of equal age, are plotted for different ages and compared to the stars of the globular cluster 47 Tucanae. Such analyses reveal that the oldest globular clusters in our Milky Way are about 12 billion years old, where different authors obtain slightly differing results—details of stellar evolution may play a role here. The age thus obtained also depends on the distance of the cluster. A revision of these distances by the Hipparcos satellite led to a decrease of the estimated ages by about two billion years. Credit: M5: ©Leos Ondra; 47 Tuc: J.E. Hesser, W.E. Harris, D.A. Vandenberg, J.W.B. Allwright, P. Scott & P.B. Stetson 1987, *A CCD color-magnitude study of 47 Tucanae*, PASP 99, 739

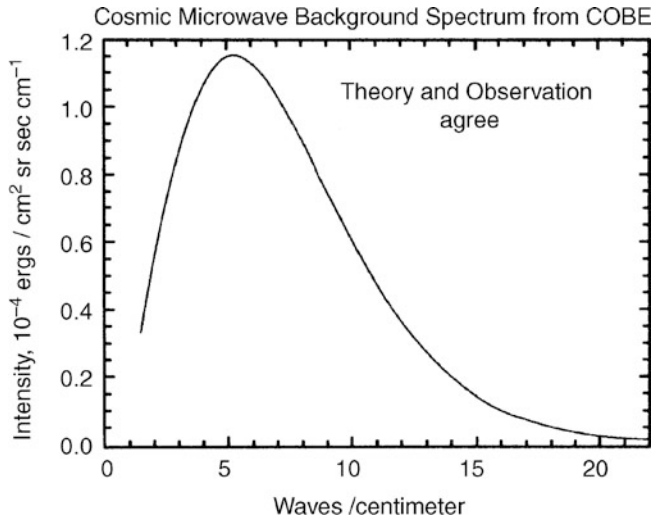


Fig. 4.3 CMB spectrum, plotted as intensity vs. frequency, measured in waves per centimeter. The solid line shows the expected spectrum of a blackbody of temperature $T = 2.728$ K. The error bars of the data, observed by the FIRAS instrument on-board COBE, are so small that the data points with error bars cannot be distinguished from the theoretical curve. Credit: COBE, NASA. We acknowledge the use of the Legacy Archive for Microwave Data Analysis (LAMBDA). Support for LAMBDA is provided by the NASA Office for Space Science

on-average homogeneous, Euclidean, static universe, and show that this assumption is in direct contradiction to observations (1) and (8).

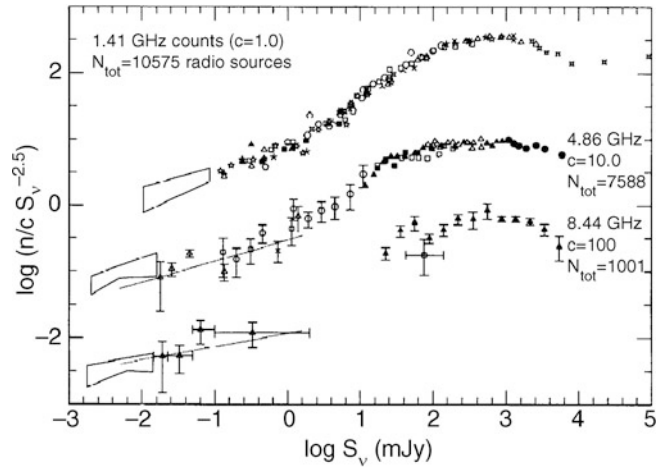


Fig. 4.4 Number counts of radio sources as a function of their flux, normalized by the Euclidean expectation $N(S) \propto S^{-5/2}$, corresponding to the integrated counts $N(> S) \propto S^{-3/2}$. Counts are displayed for three different frequencies; they clearly deviate from the Euclidean expectation. Source: R.A. Windhorst et al. 1993, *Microjansky source counts and spectral indices at 8.44 GHz*, ApJ 405, 498, p. 508, Fig. 3. ©AAS. Reproduced with permission

Olbers’ paradox (1): We can show that the night sky would be bright in such a universe—uncomfortably bright, in fact. Let n_* be the mean number density of stars, constant in space and time according to the assumptions, and let R_* be their mean radius. A spherical shell of radius r and thickness dr

around us contains $n_* dV = 4\pi r^2 dr n_*$ stars. Each of these stars subtends a solid angle of $\pi R_*^2/r^2$ on our sky, so the stars in the shell cover a total solid angle of

$$d\omega = 4\pi r^2 dr n_* \frac{R_*^2 \pi}{r^2} = 4\pi^2 n_* R_*^2 dr. \quad (4.1)$$

We see that this solid angle is independent of the radius r of the spherical shell because the solid angle covered by a single star $\propto r^{-2}$ just compensates the volume of the shell $\propto r^2$. To compute the total solid angle of all stars in a static Euclidean universe, (4.1) has to be integrated over all distances r , but the integral

$$\omega = \int_0^\infty dr \frac{d\omega}{dr} = 4\pi^2 n_* R_*^2 \int_0^\infty dr$$

diverges. Formally, this means that the stars cover an infinite solid angle, which of course makes no sense physically. The reason for this divergence is that we disregarded the effect of overlapping stellar disks on the sphere. However, these considerations demonstrate that the sky would be completely filled with stellar disks, i.e., from any direction, along any line-of-sight, light from a stellar surface would reach us. Since the specific intensity I_ν is independent of distance—the surface brightness of the Sun as observed from Earth is the same as seen by an observer who is much closer to the Solar surface—the sky would have a temperature of $\sim 10^4$ K; fortunately, this is not the case!

Source counts (8): Consider now a population of sources with a luminosity function that is constant in space and time, i.e., let $n(> L)$ be the spatial number density of sources with luminosity larger than L . A spherical shell of radius r and thickness dr around us contains $4\pi r^2 dr n(> L)$ sources with luminosity larger than L . Because the observed flux S is related to the luminosity via $L = 4\pi r^2 S$, the number of sources with flux $> S$ in this spherical shell is given as $dN(> S) = 4\pi r^2 dr n(> 4\pi r^2 S)$, and the total number of sources with flux $> S$ results from integration over the radii of the spherical shells,

$$N(> S) = \int_0^\infty dr 4\pi r^2 n(> 4\pi r^2 S).$$

Changing the integration variable to $L = 4\pi r^2 S$, or $r = \sqrt{L/(4\pi S)}$, with $dr = dL/(2\sqrt{4\pi LS})$, yields

$$\begin{aligned} N(> S) &= \int_0^\infty \frac{dL}{2\sqrt{4\pi LS}} \frac{L}{S} n(> L) \\ &\propto S^{-3/2} \int_0^\infty dL \sqrt{L} n(> L). \end{aligned} \quad (4.2)$$

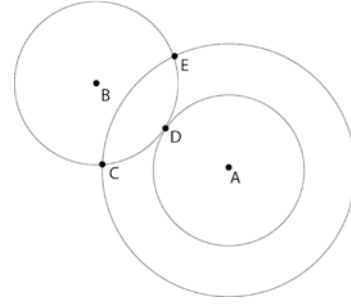


Fig. 4.5 Homogeneity follows from the isotropy around two points. If the Universe is isotropic around observer B, the densities at C, D, and E are equal. Drawing spheres of different radii around observer A, it is seen that the region within the spherical shell around A has to be homogeneous. By varying the radius of the shell, we can conclude the whole Universe must be homogeneous. Credit: J.A. Peacock 1999, *Cosmological Physics*, Cambridge University Press

From this result we deduce that the source counts in such a universe is $N(> S) \propto S^{-3/2}$, independent of the luminosity function. This is in contradiction to the observations.

From these two contradictions—Olbers' paradox and the non-Euclidean source counts—we conclude that at least one of the assumptions must be wrong. Our Universe cannot be all four of Euclidean, homogeneous, infinite, and static. The Hubble flow, i.e., the redshift of galaxies, indicates that the assumption of a static Universe is wrong.

The **age of globular clusters (5)** requires that the Universe is at least 12 Gyr old because it cannot be younger than the oldest objects it contains. Interestingly, the age estimates for globular clusters yield values which are very close to the *Hubble time* $H_0^{-1} = 9.78 h^{-1}$ Gyr. This similarity suggests that the Hubble expansion may be directly linked to the evolution of the Universe.

The apparently isotropic **distribution of galaxies (2)**, when averaged over large scales, and the **CMB isotropy (6)** suggest that the Universe around us is isotropic on large angular scales. Therefore we will first consider a world model that describes the Universe around us as isotropic. If we assume, in addition, that our place in the cosmos is not privileged over any other place, then the assumption of isotropy around us implies that the Universe appears isotropic as seen from any other place. The homogeneity of the Universe follows immediately from the isotropy around every location, as explained in Fig. 4.5. The combined assumption of homogeneity and isotropy of the Universe is also known as the *cosmological principle*. We will see that a world model based on the cosmological principle in fact provides an excellent description of numerous observational facts.

However, homogeneity is in principle unobservable because observations of distant objects show those at an earlier epoch. If the Universe evolves in time, as the

mentioned observations suggest, evolutionary effects cannot directly be separated from spatial variations.

The assumption of homogeneity of course breaks down on small scales. We observe structures in the Universe, like galaxies and clusters of galaxies, and even accumulations of clusters of galaxies, so-called superclusters. Structures have been found in redshift surveys that extend over $\sim 100 h^{-1} \text{Mpc}$. However, we have no indication of the existence of structures in the Universe with scales $\gg 100 h^{-1} \text{Mpc}$. This length-scale can be compared to a characteristic length of the Universe, which is obtained from the Hubble constant. If H_0^{-1} specifies the characteristic age of our Universe, then light will travel a distance c/H_0 in this time. With this, we have obtained in problem 1.1 the *Hubble radius* as a characteristic length-scale of the Universe (or more precisely, of the observable Universe),

$$R_H := \frac{c}{H_0} = 2998 h^{-1} \text{Mpc} : \text{Hubble radius} . \quad (4.3)$$

The Hubble volume $\sim R_H^3$ can contain a very large number of structures of size $\sim 100 h^{-1} \text{Mpc}$, so that it still makes sense to assume an on-average homogeneous cosmological model. Superposed on this homogeneous universe we then have density fluctuations that are identified with the observed large-scale structures; these will be discussed in detail in Chap. 7. To a first approximation we can neglect these density perturbations in a description of the Universe as a whole. We will therefore consider world models that are based on the cosmological principle, i.e., in which the universe looks the same for all observers (or, in other words, if observed from any point).

Homogeneous and isotropic world models are the simplest cosmological solutions of the equations of General Relativity (GR). We will examine how far such simple models are compatible with observations. As we shall see, the application of the cosmological principle results in the observational facts which were mentioned in Sect. 4.1.1.

4.2 An expanding universe

Gravitation is the fundamental force in the Universe. Only gravitational forces and electromagnetic forces can act over large distance. Since cosmic matter is electrically neutral on average, electromagnetic forces do not play any significant role on large scales, so that gravity has to be considered as the driving force in cosmology. The laws of gravity are described by the theory of General Relativity, formulated by A. Einstein in 1915. It contains Newton's theory of gravitation as a special case for weak gravitational fields and small spatial scales. Newton's theory of gravitation has been proven to be eminently successful, e.g., in describing

the motion of planets. Thus it is tempting to try to design a cosmological model based on Newtonian gravity. We will proceed to do that as a first step because not only is this Newtonian cosmology very useful from a didactic point of view, but one can also argue why the Newtonian cosmos correctly describes the major aspects of a relativistic cosmology.

4.2.1 Newtonian cosmology

The description of a gravitational system necessitates the application of GR if the length-scales in the system are comparable to the radius of curvature of spacetime; this is certainly the case in our Universe. Even if we cannot explain at this point what exactly the 'curvature radius of the Universe' is, it should be plausible that it is of the same order of magnitude as the Hubble radius R_H . We will discuss this more thoroughly further below. Despite this fact, one can expect that a Newtonian description is essentially correct: in a homogeneous universe, any small spatial region is characteristic for the whole universe. If the evolution of a small region in space is known, we also know the history of the whole universe, due to homogeneity. However, on small scales, the Newtonian approach is justified. We will therefore, based on the cosmological principle, first consider spatially homogeneous and isotropic world models in the framework of Newtonian gravity.

4.2.2 Kinematics of the Universe

Comoving coordinates. We consider a homogeneous sphere which may be radially expanding (or contracting); however, we require that the density $\rho(t)$ remains spatially homogeneous. The density may vary in time due to expansion or contraction. We choose a point $t = t_0$ in time and introduce a coordinate system \mathbf{x} at this instant with the origin coinciding with the center of the sphere. A particle in the sphere which is located at position \mathbf{x} at time t_0 will be located at some other time t at the position $\mathbf{r}(t)$ which results from the expansion of the sphere. Since the expansion is radial or, in other words, the velocity vector of a particle at position $\mathbf{r}(t)$ is parallel to \mathbf{r} , the direction of $\mathbf{r}(t)$ is constant. Because $\mathbf{r}(t_0) = \mathbf{x}$, this means that

$$\mathbf{r}(t) = a(t) \mathbf{x} . \quad (4.4)$$

Since \mathbf{x} and \mathbf{r} both have the dimension of a length, the function $a(t)$ is dimensionless; it can depend only on time. Although requiring radial expansion alone could make a depend on $|\mathbf{x}|$ as well, the requirement that the density remains homogeneous implies that a must be spatially constant. The function $a(t)$ is called the *cosmic scale factor*; due

to $\mathbf{r}(t_0) = \mathbf{x}$, it obeys

$$a(t_0) = 1. \quad (4.5)$$

The value of t_0 is arbitrary; we choose $t_0 = \text{today}$. Particles (or observers) which move according to (4.4) are called *comoving particles (observers)*, and \mathbf{x} is the comoving coordinate. The world line (\mathbf{r}, t) of a comoving observer is unambiguously determined by \mathbf{x} , $(\mathbf{r}, t) = [a(t)\mathbf{x}, t]$.

Expansion rate. The velocity of such a comoving particle is obtained from the time derivative of its position,

$$\mathbf{v}(\mathbf{r}, t) = \frac{d}{dt}\mathbf{r}(t) = \frac{da}{dt}\mathbf{x} \equiv \dot{a}\mathbf{x} = \frac{\dot{a}}{a}\mathbf{r} \equiv H(t)\mathbf{r}, \quad (4.6)$$

where in the last step we defined the *expansion rate*

$$H(t) := \frac{\dot{a}}{a}. \quad (4.7)$$

The choice of this notation is not accidental, since H is closely related to the Hubble constant. To see this, we consider the relative velocity vector of two comoving particles at positions \mathbf{r} and $\mathbf{r} + \Delta\mathbf{r}$, which follows directly from (4.6):

$$\Delta\mathbf{v} = \mathbf{v}(\mathbf{r} + \Delta\mathbf{r}, t) - \mathbf{v}(\mathbf{r}, t) = H(t)\Delta\mathbf{r}. \quad (4.8)$$

Hence, the relative velocity is proportional to the separation vector, so that the relative velocity is purely radial. Furthermore, the constant of proportionality $H(t)$ depends only on time but not on the position of the two particles. Obviously, (4.8) is very similar to the Hubble law

$$v = H_0 D, \quad (4.9)$$

in which v is the radial velocity of a source at distance D from us. Therefore, setting $t = t_0$ and $H_0 \equiv H(t_0)$, (4.8) is simply the Hubble law, in other words, (4.8) is a generalization of (4.9) for arbitrary time. It expresses the fact that any observer expanding with the sphere will observe an isotropic velocity field that follows the Hubble law. Since we are observing an expansion today—sources are moving away from us—we have $H_0 > 0$, and $\dot{a}(t_0) > 0$.

The kinematics of comoving observers in an expanding universe is analogous to that of raisins in a yeast dough. Once in the oven, the dough expands, and accordingly the positions of the raisins change. All raisins move away from all other ones, and the mutual radial velocity is proportional to the separation between any pair of raisins—i.e., their motion follows the Hubble law (4.8), with an expansion rate $H(t)$ which depends on the quality of the yeast and the temperature of the oven. The spatial position of each raisin at the time the oven is started uniquely identifies a raisin, and can be taken as its comoving coordinate \mathbf{x} , measured relative to the center of the dough. The spatial position $\mathbf{r}(t)$

at some later time t is then given by (4.4), where $a(t)$ denotes the linear size of the dough at time t relative to the size when the oven was started.

4.2.3 Dynamics of the expansion

The above discussion describes the kinematics of the expansion. However, to obtain the behavior of the function $a(t)$ in time, and thus also the motion of comoving observers and the time evolution of the density of the sphere, it is necessary to consider the dynamics. The evolution of the expansion rate is determined by self-gravity of the sphere, from which it is expected that it will cause a deceleration of the expansion.

Equation of motion. We therefore consider a spherical surface of radius x at time t_0 and, accordingly, a radius $r(t) = a(t)x$ at arbitrary time t . The mass $M(x)$ enclosed in this comoving surface is constant in time, and is given by

$$\begin{aligned} M(x) &= \frac{4\pi}{3} \rho_0 x^3 = \frac{4\pi}{3} \rho(t) r^3(t) \\ &= \frac{4\pi}{3} \rho(t) a^3(t) x^3, \end{aligned} \quad (4.10)$$

where ρ_0 must be identified with the mass density of the universe today ($t = t_0$). The density is a function of time and, due to mass conservation, it is inversely proportional to the volume of the sphere,

$$\rho(t) = \rho_0 a^{-3}(t). \quad (4.11)$$

The gravitational acceleration of a particle on the spherical surface is $GM(x)/r^2$, directed towards the center. This then yields the *equation of motion* of the particle,

$$\ddot{r}(t) \equiv \frac{d^2 r}{dt^2} = -\frac{G M(x)}{r^2} = -\frac{4\pi G}{3} \frac{\rho_0 x^3}{r^2}, \quad (4.12)$$

or, after substituting $r(t) = x a(t)$, an equation for a ,

$$\ddot{a}(t) = \frac{\ddot{r}(t)}{x} = -\frac{4\pi G}{3} \frac{\rho_0}{a^2(t)} = -\frac{4\pi G}{3} \rho(t) a(t). \quad (4.13)$$

It is important to note that this equation of motion does not depend on x . The dynamics of the expansion, described by $a(t)$, is determined solely by the matter density.

‘Conservation of energy’. Another way to describe the dynamics of the expanding shell is based on the law of energy conservation: the sum of kinetic and potential energy is constant in time. This conservation of energy is derived directly from (4.13). To do this, (4.13) is multiplied by $2\dot{a}$, and the resulting equation can be integrated with respect to time since $d(\dot{a}^2)/dt = 2\dot{a}\ddot{a}$, and $d(-1/a)/dt = \dot{a}/a^2$:

$$\dot{a}^2 = \frac{8\pi G}{3} \rho_0 \frac{1}{a} - Kc^2 = \frac{8\pi G}{3} \rho(t) a^2(t) - Kc^2; \quad (4.14)$$

here, Kc^2 is a constant of integration that will be interpreted later. After multiplication with $x^2/2$, (4.14) can be written as

$$\frac{v^2(t)}{2} - \frac{GM}{r(t)} = -Kc^2 \frac{x^2}{2},$$

which is interpreted such that the kinetic + potential energy (per unit mass) of a particle is a constant on the spherical surface. Thus (4.14) in fact describes the conservation of energy. The latter equation also immediately suggests an interpretation of the integration constant: K is proportional to the total energy of a comoving particle, and thus the history of the expansion depends on K . The sign of K characterizes the qualitative behavior of the cosmic expansion history.

- If $K < 0$, the right-hand side of (4.14) is always positive. Since $da/dt > 0$ today, da/dt remains positive for all times or, in other words, the universe will expand forever.
- If $K = 0$, the right-hand side of (4.14) is always positive, i.e., $da/dt > 0$ for all times, and the universe will also expand forever, but in a way that $da/dt \rightarrow 0$ for $t \rightarrow \infty$ —the asymptotic expansion velocity for $t \rightarrow \infty$ is zero.
- If $K > 0$, the right-hand side of (4.14) vanishes if $a = a_{\max} = (8\pi G\rho_0)/(3Kc^2)$. For this value of a , $da/dt = 0$, and the expansion will come to a halt. After that, the expansion will turn into a contraction, and such a universe will re-collapse.

In the special case of $K = 0$, which separates eternally expanding world models from those that will re-collapse in the future, the universe has a current density called *critical density* which can be inferred from (4.14) by setting $t = t_0$ and $H_0 = \dot{a}(t_0)$:

$$\rho_{\text{cr}} := \frac{3H_0^2}{8\pi G} = 1.88 \times 10^{-29} h^2 \text{ g/cm}^3. \quad (4.15)$$

Obviously, ρ_{cr} is a characteristic density of the current universe. As in many situations in physics, it is useful to express physical quantities in terms of dimensionless parameters, for instance the current cosmological density. We therefore define the *density parameter*

$$\Omega_0 := \frac{\rho_0}{\rho_{\text{cr}}}, \quad (4.16)$$

where $K > 0$ corresponds to $\Omega_0 > 1$, and $K < 0$ corresponds to $\Omega_0 < 1$. Thus, Ω_0 is one of the central cosmological parameters. Its accurate determination was possible only quite recently, and we shall discuss this in detail later. However, we should mention here that matter which is visible as stars contributes only a small fraction to the density of our Universe, $\Omega_* \lesssim 0.01$. But, as we already

discussed in the context of rotation curves of spiral galaxies and the mass determination of elliptical galaxies from the gravitational lensing effect, we find clear indications of the presence of dark matter which can in principle dominate the value of Ω_0 . We will see that this is indeed the case.

4.2.4 Modifications due to General Relativity

The Newtonian approach contains nearly all essential aspects of homogeneous and isotropic world models, otherwise we would not have discussed it in detail. Most of the above equations are also valid in relativistic cosmology, although the interpretation needs to be altered. In particular, the image of an expanding sphere needs to be revised—this picture implies that a ‘center’ of the universe exists. Such a picture implicitly contradicts the cosmological principle in which no point is singled out over others—our Universe neither has a center, nor is it expanding away from a privileged point. However, the image of a sphere does not show up in any of the relevant equations: (4.11) for the evolution of the cosmological density and (4.13) and (4.14) for the evolution of the scale factor $a(t)$ contain no quantities that refer to a sphere.

General Relativity modifies the Newtonian model in several respects:

- We know from the theory of Special Relativity that mass and energy are equivalent, according to Einstein’s famous relation $E = mc^2$. This implies that it is not only the matter density that contributes to the equations of motion. For example, a radiation field like the CMB has an energy density and, due to the equivalence above, this has to enter the expansion equations. We will see below that such a radiation field can be characterized as matter with pressure. The pressure will then explicitly appear in the equation of motion for $a(t)$.
- The field equation of GR as originally formulated by Einstein did not permit a solution which corresponds to a homogeneous, isotropic, and static cosmos. But since Einstein, like most of his contemporaries, believed the Universe to be static, he modified his field equations by introducing an additional term, the cosmological constant.
- The interpretation of the expansion is changed completely: it is not the particles or the observers that are expanding away from each other, nor is the Universe an expanding sphere. Instead, it is space itself that expands. In particular, the redshift is no Doppler redshift, but is itself a property of expanding spacetimes. However, we may still visualize redshift locally as being due to the Doppler effect without making a substantial conceptual error.²

²Returning to the picture of the raisins in a yeast dough above: On the one hand, the raisins have a velocity relative to each other, and thus

In the following, we will explain the first two aspects in more detail.

First law of thermodynamics. When air is compressed, for instance when pumping up a tire, it heats up. The temperature increases and accordingly so does the thermal energy of the air. In the language of thermodynamics, this fact is described by the first law: the change in internal energy dU through an (adiabatic) change in volume dV equals the work $dU = -P dV$, where P is the pressure in the gas. From the equations of GR as applied to a homogeneous isotropic cosmos, a relation is derived which reads

$$\frac{d}{dt} (c^2 \rho a^3) = -P \frac{da^3}{dt}, \quad (4.17)$$

in full analogy to this law. Here, ρc^2 is the energy density, i.e., for ‘normal’ matter, ρ is the mass density, and P is the pressure of the matter. If we now consider a constant comoving volume element V_x , then its physical volume $V = a^3(t) V_x$ will change due to expansion. Thus, $a^3 = V/V_x$ is the volume, and $c^2 \rho a^3$ the energy contained in the volume, each divided by V_x . Taken together, (4.17) corresponds to the first law of thermodynamics in an expanding universe.

The Friedmann–Lemaître expansion equations. Next, we will present equations for the scale factor $a(t)$ which follow from GR for a homogeneous isotropic universe. Afterwards, we will derive these equations from the relations stated above—as we shall see, the modifications by GR are in fact only minor, as expected from the argument that a small section of a homogeneous universe characterizes the cosmos as a whole. The field equations of GR yield the equations of motion

$$\left(\frac{\dot{a}}{a} \right)^2 = \frac{8\pi G}{3} \rho - \frac{Kc^2}{a^2} + \frac{\Lambda}{3} \quad (4.18)$$

and

$$\frac{\ddot{a}}{a} = -\frac{4\pi G}{3} \left(\rho + \frac{3P}{c^2} \right) + \frac{\Lambda}{3}, \quad (4.19)$$

where Λ is the aforementioned cosmological constant introduced by Einstein.³ Compared to (4.13) and (4.14), these

two equations have been changed in two places. First, the cosmological constant occurs in both equations, and second, the equation of motion (4.19) now contains a pressure term. The pair of (4.18) and (4.19) are called the *Friedmann equations*.

The cosmological constant. When Einstein introduced the Λ -term into his equations, he did this solely for the purpose of obtaining a static solution for the resulting expansion equations. We can easily see that (4.18) and (4.19), without the Λ -term, have no solution for $\dot{a} \equiv 0$. However, if the Λ -term is included, such a solution can be found (which is irrelevant, however, as we now know that the Universe is expanding). Einstein had no real physical interpretation for this constant, and after the expansion of the Universe was discovered he discarded it again. But with the genie out of the bottle, the cosmological constant remained in the minds of cosmologists, and their attitude towards Λ has changed frequently in the past 90 years. Around the turn of the millennium, observations were made which strongly suggest a non-vanishing cosmological constant, and the evidence has been further strengthened since, as will be detailed in Chap. 8. Today we know that our Universe has a non-zero cosmological constant, or at least something very similar to it.

But the physical interpretation of the cosmological constant has also been modified. In quantum mechanics even completely empty space, the so-called vacuum, may have a finite energy density, the vacuum energy density. For physical measurements not involving gravity, the value of this vacuum energy density is of no relevance since those measurements are only sensitive to energy *differences*. For example, the energy of a photon that is emitted in an atomic transition equals the energy difference between the two corresponding states in the atom. Thus the absolute energy of a state is measurable only up to a constant. Only in gravity does the absolute energy become important, because $E = mc^2$ implies that it corresponds to a mass.

It is now found that the cosmological constant is equivalent to a finite vacuum energy density—the equations of GR, and thus also the expansion equations, are not affected by this new interpretation. We will explain this fact in the following.

4.2.5 The components of matter in the Universe

Starting from the equation of energy conservation (4.14), we will now derive the relativistically correct expansion equations (4.18) and (4.19). The only change with respect to the Newtonian approach in Sect. 4.2.3 will be that we introduce other forms of matter. The essential components of our Universe can be described as pressure-free matter, radiation, and vacuum energy.

are ‘moving’. On the other hand, they are stuck in the dough, and thus have no (peculiar) velocity—they are comoving with the dough. Their mutual relative velocity thus results solely from the expansion of the dough, which can be considered an analog to the expanding spacetime.

³In the original notation, the Λ used here is denoted by Λc^2 ; for notational simplicity, we absorb the c^2 into the definition of Λ .

Pressure-free matter. The pressure in a gas is determined by the thermal motion of its constituents. At room temperature, molecules in the air move at a speed comparable to the speed of sound, $c_s \sim 300$ m/s. For such a gas, $P \sim \rho c_s^2 \ll \rho c^2$, so that its pressure is of course gravitationally completely insignificant. In cosmology, a substance with $P \ll \rho c^2$ is denoted as (pressure-free) matter, also called cosmological dust.⁴ We approximate $P_m = 0$, where the index ‘m’ stands for matter. The constituents of the (pressure-free) matter move with velocities much smaller than c .

Radiation. If this condition is no longer satisfied, thus if the thermal velocities are no longer negligible compared to the speed of light, then the pressure will also no longer be small compared to ρc^2 . In the limiting case that the thermal velocity equals the speed of light, we denote this component as ‘radiation’. One example of course is electromagnetic radiation, in particular the CMB photons. Another example would be other particles of vanishing rest mass. Even particles of finite mass can have a thermal velocity very close to c if the thermal energy of the particles is much larger than the rest mass energy, i.e., $k_B T \gg mc^2$. In these cases, the pressure is related to the density via the equation of state for radiation,

$$P_r = \frac{1}{3} \rho_r c^2 . \quad (4.20)$$

The pressure of radiation. Pressure is defined as the momentum transfer onto a perfectly reflecting wall per unit time and per unit area. Consider an isotropic distribution of photons (or another kind of particle) moving with the speed of light. The momentum of a photon is given in terms of its energy as $p = E/c = h_P \nu / c$, where h_P is the Planck constant. Consider now an area element dA of the wall; the momentum transferred to it per unit time is given by the momentum transfer per photon, times the number of photons hitting the area dA per unit time. We will assume for the moment that all photons have the same frequency. If θ denotes the direction of a photon relative to the normal of the wall, the momentum component perpendicular to the wall before scattering is $p_\perp = p \cos \theta$, and after scattering $p_\perp = -p \cos \theta$; the two other momentum components are unchanged by the reflection. Thus, the momentum transfer per photon scattering is $\Delta p = 2p \cos \theta$. The number of photons scattering per unit time within the area dA is given by the number density of photons, n_γ times the area element dA , times the thickness of the layer from which photons arrive at the wall per unit time. The latter is given by $c \cos \theta$, since only the perpendicular velocity component brings them closer to the wall. Putting these terms together, we find for the momentum transfer to the wall per unit time per unit area the expression

$$P_r(\theta) = 2 \frac{h_P \nu}{c} \cos \theta n_\gamma c \cos \theta .$$

Averaging this expression over a half-sphere (only photons moving towards the wall can hit it) then yields

$$P_r = \frac{1}{3} h_P \nu n_\gamma = \frac{1}{3} u_\gamma ,$$

where $u_\gamma = \rho_r c^2$ is the energy density of the photons. Since this final expression does not depend on the photon frequency, the assumption of a mono-chromatic distribution is not important, and the result applies to any frequency distribution.

Vacuum energy. The equation of state for vacuum energy takes a very unusual form which results from the first law of thermodynamics. Because the energy density ρ_v of the vacuum is constant in space and time, (4.17) immediately yields the relation

$$P_v = -\rho_v c^2 . \quad (4.21)$$

Thus the vacuum energy has a negative pressure. This unusual form of an equation of state can also be made plausible as follows: consider the change of a volume V that contains only vacuum. Since the internal energy is $U \propto V$, and thus a growth by dV implies an increase in U , the first law $dU = -P dV$ demands that P be negative.

4.2.6 “Derivation” of the expansion equation

Beginning with the equation of energy conservation (4.14), we are now able to derive the expansion equations (4.18) and (4.19). To achieve this, we differentiate both sides of (4.14) with respect to t and obtain

$$2 \dot{a} \ddot{a} = \frac{8\pi G}{3} (\dot{\rho} a^2 + 2 a \dot{a} \rho) .$$

Next, we carry out the differentiation in (4.17), thereby obtaining $\dot{\rho} a^3 + 3 \rho a^2 \dot{a} = -3 P a^2 \dot{a} / c^2$. This relation is then used to replace the term containing $\dot{\rho}$ in the previous equation, yielding

$$\frac{\ddot{a}}{a} = -\frac{4\pi G}{3} \left(\rho + \frac{3P}{c^2} \right) . \quad (4.22)$$

This derivation therefore reveals that the pressure term in the equation of motion results from the combination of energy conservation and the first law of thermodynamics. However, we point out that the first law in the form (4.17) is based explicitly on the equivalence of mass and energy, resulting from Special Relativity. When assuming this equivalence, we indeed obtain the Friedmann equations from Newtonian cosmology, as expected from the discussion at the beginning of Sect. 4.2.1.

Next we consider the three aforementioned components of the cosmos and write the density and pressure as the sum of dust, radiation, and vacuum energy,

$$\rho = \rho_m + \rho_r + \rho_v = \rho_{m+r} + \rho_v , \quad P = P_r + P_v ,$$

⁴The notation ‘dust’ should not be confused with the dust that is responsible for the extinction and reddening of light—‘dust’ in cosmology only denotes matter with $P = 0$.

where ρ_{m+r} combines the density in matter and radiation. In the second equation, the pressureless nature of matter, $P_m = 0$, was used so that $P_{m+r} = P_r$. By inserting the first of these equations into (4.14), we indeed obtain the first Friedmann equation (4.18) if the density ρ there is identified with ρ_{m+r} (the density in ‘normal matter’), and if

$$\rho_v = \frac{\Lambda}{8\pi G}. \quad (4.23)$$

Furthermore, we insert the above decomposition of density and pressure into the equation of motion (4.22) and immediately obtain (4.19) if we identify ρ and P with ρ_{m+r} and $P_{m+r} = P_r$, respectively. Hence, this approach yields both Friedmann equations; the density and the pressure in the Friedmann equations refer to normal matter, i.e., all matter except the contribution by Λ . Alternatively, the Λ -terms in the Friedmann equations may be discarded if instead the vacuum energy density and its pressure are explicitly included in P and ρ .

4.2.7 Discussion of the expansion equations

Following the ‘derivation’ of the expansion equations, we will now discuss their consequences. First we consider the density evolution of the various cosmic components resulting from (4.17). For pressure-free matter, we immediately obtain $\rho_m \propto a^{-3}$ which is in agreement with (4.11). Inserting the equation of state (4.20) for radiation into (4.17) yields the behavior $\rho_r \propto a^{-4}$; the vacuum energy density is a constant in time. Hence

$$\begin{aligned} \rho_m(t) &= \rho_{m,0} a^{-3}(t); \quad \rho_r(t) = \rho_{r,0} a^{-4}(t); \\ \rho_v(t) &= \rho_v = \text{const.}, \end{aligned} \quad (4.24)$$

where the index ‘0’ indicates the current time, $t = t_0$. The physical origin of the a^{-4} dependence of the radiation density is seen as follows: as for matter, the number density of photons changes $\propto a^{-3}$ because the number of photons in a comoving volume is unchanged. However, photons are redshifted by the cosmic expansion. Their wavelength λ changes proportional to a (see Sect. 4.3.2). Since the energy of a photon is $E = h\nu$ and $\nu = c/\lambda$, the energy of a photon changes as a^{-1} due to cosmic expansion so that the photon energy density changes $\propto a^{-4}$.

Analogous to (4.16), we define the dimensionless density parameters for matter, radiation, and vacuum,

$$\Omega_m = \frac{\rho_{m,0}}{\rho_{\text{cr}}}; \quad \Omega_r = \frac{\rho_{r,0}}{\rho_{\text{cr}}}; \quad \Omega_\Lambda = \frac{\rho_v}{\rho_{\text{cr}}} = \frac{\Lambda}{3H_0^2}, \quad (4.25)$$

so that $\Omega_0 = \Omega_m + \Omega_r + \Omega_\Lambda$.⁵

By now we know the current composition of our Universe quite well. The matter density of galaxies (including their dark halos) corresponds to $\Omega_m \gtrsim 0.02$, depending on the—largely unknown—extent of their dark halos. This value therefore provides a lower limit for Ω_m . Studies of galaxy clusters, which will be discussed in Chap. 6, yield a lower limit of $\Omega_m \gtrsim 0.1$. Finally, we will show in Chap. 8 that $\Omega_m \sim 0.3$.

In comparison to matter, the radiation energy density today is much smaller. The energy density of the photons in the Universe is dominated by that of the cosmic background radiation. This is even more so the case in the early Universe before the first stars have produced additional radiation. Since the CMB has a Planck spectrum of temperature 2.73 K, we know its energy density from the Stefan–Boltzmann law,

$$\begin{aligned} \rho_{\text{CMB}} &= a_{\text{SB}} T^4 \equiv \left(\frac{\pi^2 k_B^4}{15\hbar^3 c^3} \right) T^4 \\ &\simeq 4.5 \times 10^{-34} \left(\frac{T}{2.73 \text{ K}} \right)^4 \frac{\text{g}}{\text{cm}^3}, \end{aligned} \quad (4.26)$$

where in the final step we inserted the CMB temperature; here, $\hbar = h_P/(2\pi)$ is the reduced Planck constant. This energy density corresponds to a density parameter of

$$\Omega_{\text{CMB}} \simeq 2.4 \times 10^{-5} h^{-2}. \quad (4.27)$$

As will be explained below, the photons are not the only contributors to the radiation energy density. In addition, there are neutrinos from the early cosmic epoch which add to the density parameter of radiation, which then becomes

$$\Omega_r \simeq 1.68 \Omega_{\text{CMB}} \sim 4.2 \times 10^{-5} h^{-2}, \quad (4.28)$$

so that today, the energy density of radiation in the Universe can be neglected when compared to that of matter. However, (4.24) reveal that the ratio between matter and radiation density was different at earlier epochs since ρ_r evolves faster with a than ρ_m ,

$$\frac{\rho_r(t)}{\rho_m(t)} = \frac{\rho_{r,0}}{\rho_{m,0}} \frac{1}{a(t)} = \frac{\Omega_r}{\Omega_m} \frac{1}{a(t)}. \quad (4.29)$$

Thus radiation and dust had the same energy density at an epoch when the scale factor was

⁵In the literature, different definitions for Ω_0 are used. Often the notation Ω_0 is used for Ω_m .

Fig. 4.6 Two-dimensional analogies for the three possible curvatures of space. In a universe with positive curvature ($K > 0$) the sum of the angles in a triangle is larger than 180° , in a universe of negative curvature it is smaller than 180° , and in a flat universe the sum of angles is exactly 180° . Adopted from J.A. Peacock 1999, *Cosmological Physics*, Cambridge University Press



$$a_{\text{eq}} = \frac{\Omega_r}{\Omega_m} = 4.2 \times 10^{-5} (\Omega_m h^2)^{-1}. \quad (4.30)$$

This value of the scale factor and the corresponding epoch in cosmic history play a very important role in structure evolution in the Universe, as we will see in Chap. 7.

With $\rho = \rho_{m+r} = \rho_{m,0} a^{-3} + \rho_{r,0} a^{-4}$ and (4.25), the expansion equation (4.18) can be written as

$$H^2(t) = H_0^2 \left[\frac{\Omega_r}{a^4(t)} + \frac{\Omega_m}{a^3(t)} - \frac{Kc^2}{H_0^2 a^2(t)} + \Omega_\Lambda \right]. \quad (4.31)$$

Evaluating this equation at the present epoch, with $H(t_0) = H_0$ and $a(t_0) = 1$, yields the value of the integration constant K ,

$$\begin{aligned} K &= \left(\frac{H_0}{c} \right)^2 (\Omega_0 - 1) = \left(\frac{H_0}{c} \right)^2 (\Omega_m + \Omega_\Lambda + \Omega_r - 1) \\ &\approx \left(\frac{H_0}{c} \right)^2 (\Omega_m + \Omega_\Lambda - 1). \end{aligned} \quad (4.32)$$

Hence the constant K is obtained from the density parameters, mainly those of matter and vacuum since $\Omega_r \ll \Omega_m$, and has the dimension of $(\text{length})^{-2}$. In the context of GR, K is interpreted as the curvature scalar of the universe today, or more precisely, the homogeneous, isotropic three-dimensional space at time $t = t_0$ has a curvature K . Depending on the sign of K , we can distinguish the following cases:

- If $K = 0$, the three-dimensional space for any fixed time t is Euclidean, i.e., flat.
- If $K > 0$, $1/\sqrt{K}$ can be interpreted as the curvature radius of the spherical 3-space—the two-dimensional analogy would be the surface of a sphere. As already speculated in Sect. 4.2.1, the order of magnitude of the curvature radius is c/H_0 according to (4.32).

- If $K < 0$, the space is called hyperbolic—the two-dimensional analogy would be the surface of a saddle (see Fig. 4.6).

Hence GR provides a relation between the curvature of space and the density of the universe. In fact, this is the central aspect of GR which links the geometry of spacetime to its matter content. However, Einstein's theory makes no statement about the topology of spacetime and, in particular, says nothing about the topology of the universe.⁶ If the universe has a simple topology, it is finite in the case of $K > 0$, whereas it is infinite if $K \leq 0$. However, in both cases it has no boundary (compare: the surface of a sphere is a finite space without boundaries).

With (4.31) and (4.32), we finally obtain the expansion equation in the form

$$\begin{aligned} \left(\frac{\dot{a}}{a} \right)^2 &= H^2(t) \\ &= H_0^2 \left[\frac{\Omega_r}{a^4(t)} + \frac{\Omega_m}{a^3(t)} + \frac{(1-\Omega_m-\Omega_\Lambda)}{a^2(t)} + \Omega_\Lambda \right], \\ &\equiv H_0^2 E^2(t) \end{aligned} \quad (4.33)$$

where in the final step we defined the dimensionless Hubble function $E(t) = H(t)/H_0$ for later purposes.

4.3 Consequences of the Friedmann expansion

The cosmic expansion equations imply a number of immediate consequences, some of which will be discussed next. In particular, we will first demonstrate that the early Universe

⁶The surface of a cylinder is also considered a flat space, like a plane, because the sum of angles in a triangle on a cylinder is also 180° . But the surface of a cylinder obviously has a topology different from a plane; in particular, closed straight lines do exist—walking on a cylinder in a direction perpendicular to its axis, one will return to the starting point after a finite amount of time.

must have evolved out of a very dense and hot state called the *Big Bang*. We will then link the scale factor a to an observable, the redshift, and explain what the term ‘distance’ means in cosmology.

4.3.1 The necessity of a Big Bang

The terms on the right-hand side of (4.33) each have a different dependence on a :

- For very small a , the first term dominates and the universe is dominated by radiation then.
- For slightly larger $a \gtrsim a_{\text{eq}}$, the pressureless matter (dust) term dominates.
- If $K \neq 0$, the third term, also called the curvature term, can dominate for larger a .
- For even larger a , the cosmological constant dominates if it is different from zero.

The differential equation (4.33) in general cannot be solved analytically. However, its numerical solution for $a(t)$ poses no problems. Nevertheless, we can analyze the qualitative behavior of the function $a(t)$ and thereby understand the essential aspects of the expansion history. From the Hubble law, we conclude that $\dot{a}(t_0) > 0$, i.e., a is currently an increasing function of time. Equation (4.33) shows that $\dot{a}(t) > 0$ for all times, unless the right-hand side of (4.33) vanishes for some value of a : the sign of \dot{a} can only switch when the right-hand side of (4.33) is zero. If $H^2 = 0$ for a value of $a > 1$, the expansion will come to a halt and the Universe will recollapse afterwards. On the other hand, if $H^2 = 0$ for a value $a = a_{\text{min}}$ with $0 < a_{\text{min}} < 1$, then the sign of \dot{a} switches at a_{min} . At this epoch, a collapsing Universe changes into an expanding one.

Classification of model. Which of these alternatives describes our Universe depends on the density parameters. We find the following classification (also see Fig. 4.7 and problem 4.3):

- If $\Lambda = 0$, then $H^2 > 0$ for all $a \leq 1$, whereas the behavior for $a > 1$ depends on Ω_m :
 - if $\Omega_m \leq 1$ (or $K \leq 0$, respectively), $H^2 > 0$ for all a : the universe will expand for all times. This behavior is expected from the Newtonian approach because if $K \leq 0$, the kinetic energy in any spherical shell is larger than the modulus of the potential energy, i.e., the expansion velocity exceeds the escape velocity and the expansion will never come to a halt.
 - If $\Omega_m > 1$ ($K > 0$), H^2 will vanish for $a = a_{\text{max}} = \Omega_m/(\Omega_m - 1)$. The universe will have its maximum expansion when the scale factor is a_{max} and will recollapse thereafter. In Newtonian terms, the total energy of any spherical shell is negative, so that it is gravitationally bound.

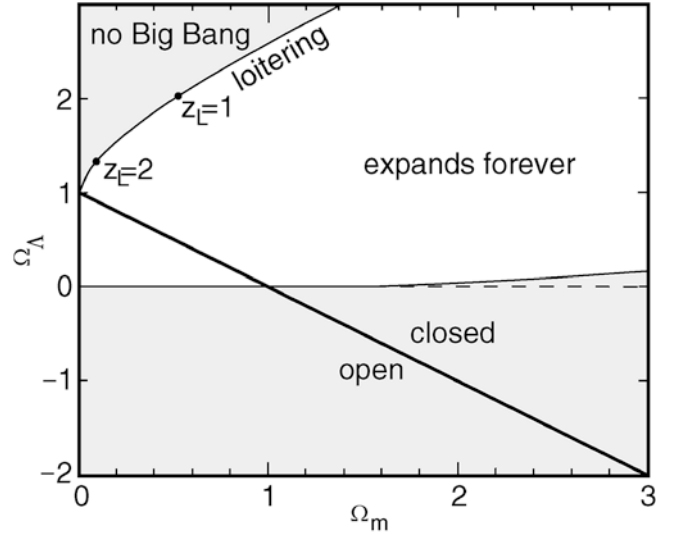


Fig. 4.7 Classification of cosmological models. The *straight solid line* connects flat models (i.e., those without spatial curvature, $\Omega_m + \Omega_\Lambda = 1$) and separates open ($K < 0$) and closed ($K > 0$) models. The nearly horizontal curve separates models that will expand forever from those that will recollapse in the distant future. Models in the upper left corner have an expansion history where a has never been close to zero and thus did not experience a Big Bang. In those models, a maximum redshift for sources exists, which is indicated for two cases. Since we know that $\Omega_m > 0.1$, and sources at redshift > 6 have been observed, these models can be excluded. Adopted from J.A. Peacock 1999, *Cosmological Physics*, Cambridge University Press

We thus have reobtained the classification discussed before in Sect. 4.2.3, which is valid for $\Lambda = 0$, for which the qualitative behavior of the expansion depends only on the sign of K .

- In the presence of a cosmological constant $\Lambda > 0$, the discussion becomes more complicated; in particular, the geometry of the universe, i.e., the sign of K , is not sufficient to predict the qualitative expansion behavior. For example, there are models with positive curvature (indicated as ‘closed’ in Fig. 4.7) which expand forever. One finds for $\Lambda \geq 0$:
 - If $\Omega_m < 1$, the universe will expand for all $a > 1$.
 - However, for $\Omega_m > 1$ the future behavior of $a(t)$ depends on Ω_Λ : if Ω_Λ is sufficiently small, a value a_{max} exists at which the expansion comes to a halt and reverses. In contrast, if Ω_Λ is large enough the universe will expand forever.
 - If $\Omega_\Lambda < 1$, then $H^2 > 0$ for all $a \leq 1$.
 - However, if $\Omega_\Lambda > 1$, it is in principle possible that $H^2 = 0$ for an $a = a_{\text{min}} < 1$. Such models, in which a minimum value for a existed in the past (so-called bouncing models), can be excluded by observations (see Sect. 4.3.2).

With the exception of the last case, which can be excluded, we come to the conclusion that a must have attained the

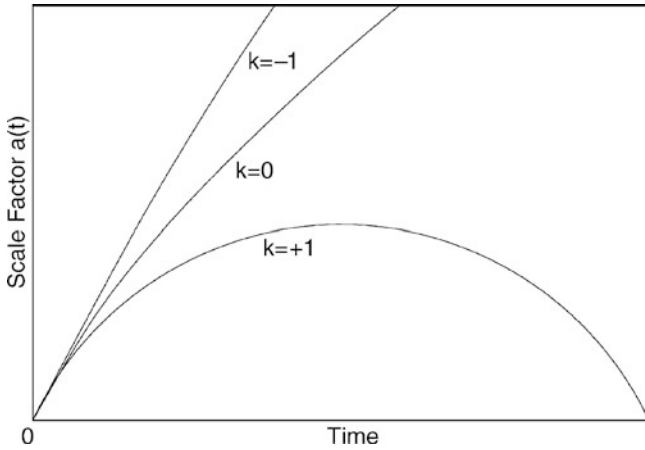


Fig. 4.8 The scale factor $a(t)$ as a function of cosmic time t for three models with a vanishing cosmological constant, $\Omega_\Lambda = 0$. Closed models ($K > 0$) attain a maximum expansion and then recollapse. In contrast, open models ($K \leq 0$) expand forever, and the Einstein–de Sitter model of $K = 0$ separates these two cases. In all models, the scale factor tends towards zero in the past; this time is called the Big Bang and defines the origin of the time axis

value $a = 0$ at some point in the past, at least formally. At this instant the ‘size of the Universe’ formally vanished. As $a \rightarrow 0$, both matter and radiation densities diverge so that the density in this state must have been singular. The epoch at which $a = 0$ and the evolution away from this state is called the *Big Bang*. It is useful to define this epoch ($a = 0$) as the origin of time, so that t is identified with the age of the Universe, the time since the Big Bang. As we will show, the predictions of the Big Bang model are in impressive agreement with observations.

The expansion history for the special case of a vanishing vacuum energy density is sketched in Fig. 4.8 for three values of the curvature.

To characterize whether the current expansion of the Universe is decelerated or accelerated, the *deceleration parameter*

$$q_0 := -\ddot{a} a / \dot{a}^2 \quad (4.34)$$

is defined where the right-hand side has to be evaluated at $t = t_0$. With (4.19) and (4.33) it follows that

$$q_0 = \Omega_m / 2 - \Omega_\Lambda. \quad (4.35)$$

If $\Omega_\Lambda = 0$ then $q_0 > 0$, $\ddot{a} < 0$, i.e., the expansion decelerates, as expected due to gravity. However, if Ω_Λ is sufficiently large the deceleration parameter may become negative, corresponding to an accelerated expansion of the universe. The reason for this behavior, which certainly contradicts intuition, is seen in the vacuum energy. Only a negative pressure can cause an accelerated expansion—more precisely, as seen from (4.22), $P < -\rho c^2/3$ is needed for $\ddot{a} > 0$. Indeed, we know today that our Universe is

currently undergoing an accelerated expansion and thus that the cosmological constant differs significantly from zero.

Age of the universe. The age of the universe at a given scale factor a follows from $dt = da(da/dt)^{-1} = da/(aH)$. This relation can be integrated,

$$t(a) = \frac{1}{H_0} \int_0^a dx \left[x^{-2} \Omega_r + x^{-1} \Omega_m + (1 - \Omega_m - \Omega_\Lambda) + x^2 \Omega_\Lambda \right]^{-1/2}, \quad (4.36)$$

where the contribution from radiation for $a \gg a_{\text{eq}}$ can be neglected because it is relevant only for very small a and thus only for a very small fraction of cosmic time. To obtain the current age t_0 of the universe, (4.36) is calculated for $a = 1$. For models of vanishing spatial curvature $K = 0$ and for those with $\Lambda = 0$, Fig. 4.9 displays t_0 as a function of Ω_m .

The qualitative behavior of the cosmological models is characterized by the density parameters Ω_m and Ω_Λ , whereas the Hubble constant H_0 determines ‘only’ the overall length- or time-scale. One can consider several special cases for the density parameters:

- Models without a cosmological constant, $\Lambda = 0$. The difficulties in deriving a ‘sensible’ value for Λ from particle physics has in the past often been used as an argument for neglecting the vacuum energy density. However, there are now very strong observational indications that in fact $\Lambda > 0$.
- Models with $\Omega_m + \Omega_\Lambda = 1$, i.e., $K = 0$. Such flat models are preferred by the so-called inflationary models, which we will briefly discuss further below.
- A special case is the Einstein–de Sitter model, $\Omega_m = 1$, $\Omega_\Lambda = 0$. For this model, $t_0 = 2/(3H_0) \approx 6.7 h^{-1} \times 10^9 \text{ yr}$.
- For many world models, t_0 is larger than the age of the oldest globular clusters, so they are compatible with this age determination. The Einstein–de Sitter model, however, is compatible with stellar ages only if H_0 is very small, considerably smaller than the value of H_0 derived from the HST Key Project discussed in Sect. 3.9. Hence, this model is ruled out by these observations.

The values of the cosmological parameters are now quite well known. We list them here for later reference without any further discussion. Their determination will be described in the course of this chapter and in Chap. 8. The values are approximately

$$\boxed{\Omega_m \sim 0.3; \Omega_\Lambda \sim 0.7; h \sim 0.7}. \quad (4.37)$$

Early expansion. In the early phase of the universe, the curvature term and the vacuum energy density can be neglected in the expansion

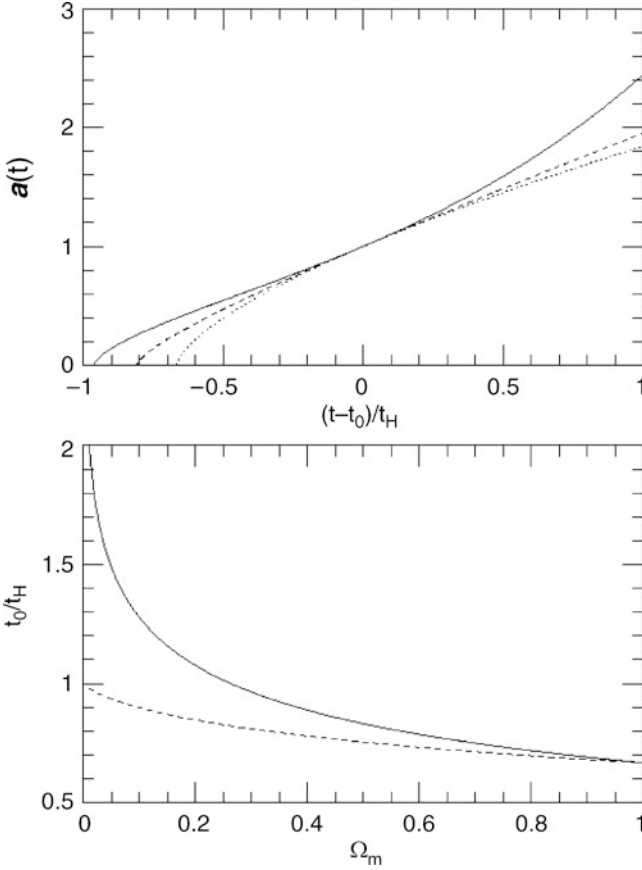


Fig. 4.9 *Top panel:* Scale factor $a(t)$ as a function of cosmic time, here scaled as $(t-t_0)H_0$, for an Einstein-de Sitter model ($\Omega_m = 1, \Omega_\Lambda = 0$; dotted curve), an open universe ($\Omega_m = 0.3, \Omega_\Lambda = 0$; dashed curve), and a flat universe of low density ($\Omega_m = 0.3, \Omega_\Lambda = 0.7$; solid curve). At the current epoch, $t = t_0$ and $a = 1$. *Bottom panel:* Age of the universe in units of the Hubble time $t_H = H_0^{-1}$ for flat world models with $K = 0$ ($\Omega_m + \Omega_\Lambda = 1$; solid curve) and models with a vanishing cosmological constant (dashed curve). We see that for a flat universe with small Ω_m (thus large $\Omega_\Lambda = 1 - \Omega_m$), t_0 may be considerably larger than H_0^{-1} . Credit: M. Bartelmann, MPA Garching

equation (4.33), which then simplifies to

$$H^2 = H_0^2 \left(\frac{\Omega_r}{a^4} + \frac{\Omega_m}{a^3} \right) = H_0^2 \Omega_m a^{-3} \left(1 + \frac{a_{\text{eq}}}{a} \right),$$

where we used (4.30). In this case, the relation (4.36) between time and scale factor can be integrated explicitly to yield

$$t = \frac{2}{3H_0\sqrt{\Omega_m}} \left[a^{3/2} \left(1 - \frac{2a_{\text{eq}}}{a} \right) \sqrt{1 + \frac{a_{\text{eq}}}{a}} + 2a_{\text{eq}}^{3/2} \right]. \quad (4.38)$$

From this result we can infer that the scale factor behaves at $a \propto t^{1/2}$ for $a \ll a_{\text{eq}}$ and that $a \propto t^{2/3}$ in the matter dominated era.

4.3.2 Redshift

The Hubble law describes a relation between the redshift, or the radial component of the relative velocity, and the distance of an object from us. Furthermore, (4.6) specifies

that any observer is experiencing a local Hubble law with an expansion rate $H(t)$ which depends on the cosmic epoch. We will now derive a relation between the redshift of a source, which is directly observable, and the cosmic time t or the scale factor $a(t)$, respectively, at which the source emitted the light we receive today.

To do this, we consider a light ray that reaches us today. Along this light ray we imagine fictitious comoving observers. The light ray is parametrized by the cosmic time t , and is supposed to have been emitted by the source at epoch t_e . Two comoving observers along the light ray with separation dr from each other see their relative motion due to the cosmic expansion according to (4.6), $dv = H(t) dr$, and they measure it as a redshift of light, $d\lambda/\lambda = dz = dv/c$. It takes a time $dt = dr/c$ for the light to travel from one observer to the other. Furthermore, from the definition of the Hubble parameter, $\dot{a} = da/dt = H a$, we obtain the relation $dt = da/(H a)$. Combining these relations, we find

$$\frac{d\lambda}{\lambda} = \frac{dv}{c} = \frac{H}{c} dr = H dt = \frac{da}{a}. \quad (4.39)$$

The relation $d\lambda/\lambda = da/a$ is now easily integrated since the equation $d\lambda/da = \lambda/a$ obviously has the solution $\lambda = Ca$, where C is a constant. That constant is determined by the wavelength λ_{obs} of the light as observed today (i.e., at $a = 1$), so that

$$\lambda(a) = a \lambda_{\text{obs}}. \quad (4.40)$$

The wavelength at emission was therefore $\lambda_e = a(t_e)\lambda_{\text{obs}}$. On the other hand, the redshift z is defined as $(1+z) = \lambda_{\text{obs}}/\lambda_e$. From this, we finally obtain the relation

$$1+z = \frac{1}{a} \quad (4.41)$$

between the observable z and the scale factor a which is linked via (4.36) to the cosmic time. The same relation can also be derived by considering light rays in GR.

The relation between redshift and the scale factor is of immense importance for cosmology because, for most sources, redshift is the only distance information that we are able to measure. If the scale factor is a monotonic function of time, i.e., if the right-hand side of (4.33) is different from zero for all $a \in [0, 1]$, then z is also a monotonic function of t . In this case, which corresponds to the Universe we happen to live in, a , t , and z are equally good measures of the distance of a source from us.

Local Hubble law. The Hubble law applies for nearby sources: with (4.8) and $v \approx zc$ it follows that

$$z = \frac{H_0}{c} D \approx \frac{h D}{3000 \text{ Mpc}} \text{ for } z \ll 1, \quad (4.42)$$

where D is the distance of a source with redshift z . This corresponds to a light travel time of $\Delta t = D/c$. On the other hand, due to the definition of the Hubble parameter, we have $\Delta a = (1 - a) \approx H_0 \Delta t$, where a is the scale factor at time $t_0 - \Delta t$, and we used $a(t_0) = 1$ and $H(t_0) = H_0$. This implies $D = (1 - a)c/H_0$. Utilizing (4.42), we then find $z = 1 - a$, or $a = 1 - z$, which agrees with (4.41) in linear approximation since $(1 + z)^{-1} = 1 - z + \mathcal{O}(z^2)$. Hence we conclude that the general relation (4.41) contains the local Hubble law as a special case.

Energy density in radiation. A further consequence of (4.41) is the dependence of the energy density of radiation on the scale parameter. As mentioned previously, the number density of photons is $\propto a^{-3}$ if we assume that photons are neither created nor destroyed. In other words, the number of photons in a comoving volume element is conserved. According to (4.41), the frequency ν of a photon changes due to cosmic expansion. Since the energy of a photon is $\propto \nu$, $E_\gamma = h_P \nu \propto 1/a$, the energy density of photons decreases, $\rho_r \propto n E_\gamma \propto a^{-4}$. Therefore (4.41) implies (4.24).

Cosmic microwave background. Assuming that, at some time t_1 , the universe contained a blackbody radiation of temperature T_1 , we can examine the evolution of this photon population in time by means of relation (4.41). We should recall that the Planck function B_ν (A.13) specifies the radiation energy of blackbody radiation that passes through a unit area per unit time, per unit frequency interval, and per unit solid angle. Using this definition, the number density dN_ν of photons in the frequency interval between ν and $\nu + d\nu$ is obtained as

$$\frac{dN_\nu}{d\nu} = \frac{4\pi B_\nu}{c h_P \nu} = \frac{8\pi \nu^2}{c^3} \frac{1}{\exp\left(\frac{h_P \nu}{k_B T_1}\right) - 1}. \quad (4.43)$$

At a later time $t_2 > t_1$, the universe has expanded by a factor $a(t_2)/a(t_1)$. An observer at t_2 therefore observes the photons redshifted by a factor $(1 + z) = a(t_2)/a(t_1)$, i.e., a photon with frequency ν at t_1 will then be measured to have frequency $\nu' = \nu/(1 + z)$. The original frequency interval is transformed accordingly as $d\nu' = d\nu/(1 + z)$. The number density of photons decreases with the third power of the scale factor, so that $dN'_{\nu'} = dN_\nu/(1 + z)^3$. Combining these relations, we obtain for the number density $dN'_{\nu'}$ of photons in the frequency interval between ν' and $\nu' + d\nu'$

$$\begin{aligned} \frac{dN'_{\nu'}}{d\nu'} &= \frac{dN_\nu/(1 + z)^3}{d\nu/(1 + z)} \\ &= \frac{1}{(1 + z)^2} \frac{8\pi(1 + z)^2 \nu'^2}{c^3} \frac{1}{\exp\left(\frac{h_P(1 + z)\nu'}{k_B T_1}\right) - 1} \end{aligned}$$

$$= \frac{8\pi \nu'^2}{c^3} \frac{1}{\exp\left(\frac{h_P \nu'}{k_B T_2}\right) - 1}, \quad (4.44)$$

where we used $T_2 = T_1/(1 + z)$ in the last step. The distribution (4.44) has the same form as (4.43) except that the temperature is reduced by a factor $(1 + z)^{-1}$. If a Planck distribution of photons had been established at an earlier time, it will persist during cosmic expansion. As we have seen above, the CMB is such a blackbody radiation, with a current temperature of $T_0 = T_{\text{CMB}} \approx 2.73$ K. We will show in Sect. 4.4 that this radiation originates in the early phase of the cosmos. Thus it is meaningful to consider the temperature of the CMB as the ‘temperature of our Universe’ which is a function of redshift,

$$T(z) = T_0(1 + z) = T_0 a^{-1}, \quad (4.45)$$

i.e., the Universe was hotter in the past than it is today. The energy density of the Planck spectrum is given by (4.26), i.e., proportional to T^4 , so that ρ_r behaves like $(1 + z)^4 = a^{-4}$ in accordance with (4.24).⁷

Finally, it should be stressed again that (4.41) allows all relations to be expressed as functions of a as well as of z . For example, the age of the Universe as a function of z is obtained by replacing the upper integration limit, $a \rightarrow (1 + z)^{-1}$, in (4.36).

Interpretation of cosmological redshift. The redshift results from the fact that during the expansion of the universe, the energy of the photons decreases in proportion to $1/a$, which is the reason, together with the decreasing proper number density, that $\rho_r(a) \propto a^{-4}$. Our considerations in this section have derived this $1/a$ -dependence of the photon energy.

But maybe this is puzzling anyway—if photons lose energy during cosmic expansion, then, having in mind the concept of energy conservation, one might be tempted to ask: Where does this energy go to?

To answer this question, we start with pointing out that energy conservation in cosmology is expressed by the ‘first law of thermodynamics’ (4.17), which has as one of its consequences the $1/a$ -behavior of photon energy. Thus, there is no reason to lose sleep about this issue.

But it may be useful to be more explicit here. We first point out that ‘the energy’ of a photon, or any other particle,

⁷Generally, it can be shown that the specific intensity I_ν changes due to redshift according to

$$\frac{I_\nu}{\nu^3} = \frac{I'_{\nu'}}{(\nu')^3}. \quad (4.46)$$

Here, I_ν is the specific intensity today at frequency ν and $I'_{\nu'}$ is the specific intensity at redshift z at frequency $\nu' = (1 + z)\nu$.

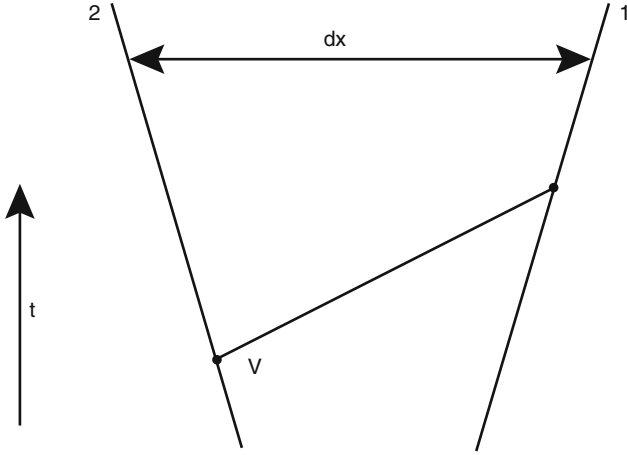


Fig. 4.10 Sketch of two comoving observers with comoving separation dx , and a particle with velocity v , as measured by observer No. 2, moving from the worldline of observer No. 2 to that of observer No. 1

as such is not defined! To see this, consider two observers that measure the wavelength of photons; both are at the same location, but observer No. 2 moves in the direction of the light source, as seen from observer No. 1. Because of the Doppler effect, observer No. 2 measures a shorter wavelength than observer No. 1; thus, the two observers come to different conclusions about the energy of the photons. It's not like one of them is right, the other wrong—the energy of a photon is not an absolute quantity, but depends on the frame in which it is measured.

We have defined a reference frame in an expanding universe, that of comoving observers—they are the ones who see the universe being isotropic around them. When we state that ‘the photon energy changes as $1/a$ ’, we implicitly mean that it is the energy as measured by the comoving observer that changes. As these comoving observers move relative to each other, as expressed by the Hubble law, it should not be a surprise that they measure different frequencies of photons, as explicitly accounted for in (4.39). Thus, not the properties of the photons are changing in time, but the state of motion of the observers that measure the photon energy as they propagate through the universe.

In fact, one can show that in general the momentum (as measured by comoving observers!) of a freely moving particle changes as

$$p \propto \frac{1}{a}. \quad (4.47)$$

For photons, we have already shown this: since the momentum of a photon is given by its energy, divided by c , then $v \propto 1/a$ shows the validity of (4.47). The same is true for other relativistic particles as well. We can also derive this behavior easily for non-relativistic particles. Consider a particle of mass m which crosses the worldlines of the two neighboring observers 2 and 1 (see Fig. 4.10). Let dx

be their comoving separation, then at epoch a their physical separation is $dr = a dx$. It takes the particle the time $dt = dr/v$ to travel between the two observers, where v is the velocity measured by observer No. 2. Observer No. 1 will measure a velocity $v - dv$, since from his perspective, observer No. 2 is receding from him (this is simply a Galilean transformation), with a velocity $dv = H(a) dr$ given by the local Hubble law. Putting this together, there is a momentum change $dp = -m dv$ of the particle when measured by the two observers, where

$$\frac{dp}{p} = -\frac{H(a) dr}{v} = -H(a) dt = -\frac{da/dt}{a} dt = -\frac{da}{a}, \quad (4.48)$$

where we made use of the definition of the Hubble function. The resulting equation $d \ln p = -d \ln a$ has the solution $pa = \text{const.}$, i.e., (4.47) holds. For semi-relativistic particles, the proof of (4.47) can be made with Special Relativity, but proceeds essentially in the same way.

The necessity of a Big Bang. We discussed in Sect. 4.3.1 that the scale factor must have attained the value $a = 0$ at some time in the past. One gap in our argument that inevitably led to the necessity of a Big Bang still remains, namely the possibility that at some time in the past $\dot{a} = 0$ occurred, i.e., that the universe underwent a transition from a contracting to an expanding state. This is possible only if $\Omega_\Lambda > 1$ and if the matter density parameter is sufficiently small (see Fig. 4.7). In this case, a attained a minimum value in the past. This minimum value depends on both Ω_m and Ω_Λ . For instance, for $\Omega_m > 0.1$, the value is $a_{\min} \gtrsim 0.3$. But a minimum value for a implies a maximum redshift $z_{\max} = 1/a_{\min} - 1$. However, since we have observed quasars and galaxies with $z > 6$ and the density parameter is known to be $\Omega_m > 0.1$, such a model without a Big Bang can be safely excluded.

4.3.3 Distances in cosmology

In the previous sections, different distance measures were discussed. Because of the monotonic behavior of the corresponding functions, each of a , t , and z provide the means to sort objects according to their distance. An object at higher redshift z_2 is more distant than one at $z_1 < z_2$ such that light from a source at z_2 may become absorbed by gas in an object at redshift z_1 , but not vice versa. The object at redshift z_1 is located between us and the object at z_2 . The more distant a source is from us, the longer the light takes to reach us, the earlier it was emitted, the smaller a was at emission, and the larger z is. Since z is the only observable of these parameters, distances in extragalactic astronomy are nearly always expressed in terms of redshift.

But how can a redshift be translated into a distance that has the dimension of a length? Or, phrasing this question differently, how many Megaparsecs away from us is a source with redshift $z = 2$? The corresponding answer is more complicated than the question suggests. For very small redshifts, the local Hubble relation (4.42) may be used, but this is valid only for $z \ll 1$.

In a static Euclidean space, the separation between two points is unambiguously defined, and several prescriptions exist for measuring a distance. We will give two examples here. A sphere of radius R situated at distance D subtends a solid angle of $\omega = \pi R^2/D^2$ on our sky. If the radius is known, D can be measured using this relation. As a second example, we consider a source of luminosity L at distance D which then has a measured flux $S = L/(4\pi D^2)$. Again, if the luminosity is known, the distance can be computed from the observed flux. If we use these two methods to determine, for example, the distance to the Sun, we would of course obtain identical results for the distance (within the range of accuracy), since these two prescriptions for distance measurements are defined to yield equal results.

In a non-Euclidean or expanding/contracting space-time like, for instance, our Universe this is no longer the case. The equivalence of different distance measures is only ensured in Euclidean space, and we have no reason to expect this equivalence to also hold in a curved spacetime. In cosmology, the same measuring prescriptions as in Euclidean space are used for defining distances, but the different definitions lead to different results. The two most important definitions of distance are:

- **Angular-diameter distance:** As above, we consider a source of radius R observed to cover a solid angle ω . The angular-diameter distance is defined as

$$D_A(z) = \sqrt{\frac{R^2 \pi}{\omega}}. \quad (4.49)$$

- **Luminosity distance:** We consider a source with bolometric luminosity L and flux S and define its luminosity distance as

$$D_L(z) = \sqrt{\frac{L}{4\pi S}}. \quad (4.50)$$

These two distances agree locally, i.e., for $z \ll 1$; on small scales, the curvature of spacetime is not noticeable. In addition, they are *unique* functions of redshift. They can be computed explicitly. However, to do this some tools of GR are required. Since we have not discussed GR in this book, these tools are not available to us here. The distance-redshift relations depend on the cosmological parameters; Fig. 4.11 shows the angular-diameter distance for different models. For $\Lambda = 0$, the famous Mattig relation applies,

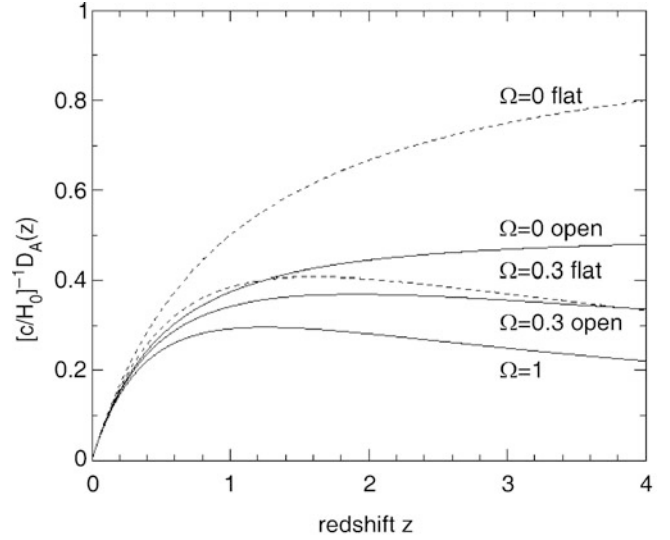


Fig. 4.11 Angular-diameter distance vs. redshift for different cosmological models. *Solid curves* display models with no vacuum energy; *dashed curves* show flat models with $\Omega_m + \Omega_\Lambda = 1$. In both cases, results are plotted for $\Omega_m = 1, 0.3$, and 0 . Adopted from J.A. Peacock 1999, *Cosmological Physics*, Cambridge University Press

$$D_A(z) = \frac{c}{H_0} \frac{2}{\Omega_m^2 (1+z)^2} \times \left[\Omega_m z + (\Omega_m - 2) \left(\sqrt{1 + \Omega_m z} - 1 \right) \right]. \quad (4.51)$$

In particular, D_A is not necessarily a monotonic function of z . To better comprehend this, we consider the geometry on the surface of a sphere. Two great circles on Earth are supposed to intersect at the North Pole enclosing an angle $\varphi \ll 1$ —they are therefore meridians. The separation L between these two great circles, i.e., the length of the connecting line perpendicular to both great circles, can be determined as a function of the distance D from the North Pole, which is measured as the distance along one of the two great circles. If θ is the geographical latitude ($\theta = \pi/2$ at the North Pole, $\theta = -\pi/2$ at the South Pole), $L = R\varphi \cos \theta$ is found, where R is the radius of the Earth. L vanishes at the North Pole, attains its maximum at the equator (where $\theta = 0$), and vanishes again at the South Pole; this is because both meridians intersect there again. Furthermore, $D = R(\pi/2 - \theta)$, e.g., the distance to the equator $D = R\pi/2$ is a quarter of the Earth's circumference. Solving the last relation for θ , the distance is then given by $L = R\varphi \cos(\pi/2 - D/R) = R\varphi \sin(D/R)$. For the angular-diameter distance on the Earth's surface, we define $D_A(D) = L/\varphi = R \sin(D/R)$, in analogy to the definition (4.49). For values of D that are considerably smaller than the curvature radius R of the sphere, we therefore obtain that $D_A \approx D$, whereas for larger D , D_A deviates considerably from D . In particular, D_A is not a monotonic

function of D , rather it has a maximum at $D = \pi R/2$ and then decreases for larger D .

There exists a general relation between angular-diameter distance and luminosity distance,

$$D_L(z) = (1+z)^2 D_A(z). \quad (4.52)$$

The reader might now ask which of these distances is the *correct one*? Well, this question does not make sense since there is no unique definition of the distance in a curved spacetime like our Universe. Instead, the aforementioned measurement prescriptions must be used. The choice of a distance definition depends on the desired application of this distance. For example, if we want to compute the linear diameter of a source with observed angular diameter, the angular-diameter distance must be employed because it is defined just in this way. On the other hand, to derive the luminosity of a source from its redshift and observed flux, the luminosity distance needs to be applied. Due to the definition of the angular-diameter distance (length/angular diameter), those are the relevant distances that appear in the gravitational lens equation (3.63). A statement that a source is located “at a distance of 7 billion light years” away from us is meaningless unless it is mentioned which type of distance is meant. Again, in the low-redshift Universe ($z \ll 1$), the differences between different distance definitions are very small, and thus it is meaningful to state, for example, that the Coma cluster of galaxies lies at a distance of ~ 90 Mpc.

In Fig. 4.12 a Hubble diagram extending to high redshifts is shown, where the brightest galaxies in clusters of galaxies have been used as approximate standard candles. With an assumed constant intrinsic luminosity for these galaxies, the apparent magnitude is a measure of their distance, where the luminosity distance $D_L(z)$ must be applied to compute the flux as a function of redshift.

We compile several expressions that are required to compute distances in general Friedmann–Lemaître models (see also problem 4.6). To do this, we need to define the function

$$f_K(x) = \begin{cases} 1/\sqrt{K} \sin(\sqrt{K}x) & K > 0 \\ x & K = 0 \\ 1/\sqrt{-K} \sinh(\sqrt{-K}x) & K < 0 \end{cases},$$

where K is the curvature scalar (4.32). The comoving radial distance x of a source at redshift z can be computed using $dx = a^{-1} dr = -a^{-1} c dt = -c da/(a^2 H)$. Hence with (4.33)

$$x(z) = \int_{(1+z)^{-1}}^1 \frac{da (c/H_0)}{\sqrt{a\Omega_m + a^2(1-\Omega_m-\Omega_\Lambda) + a^4\Omega_\Lambda}}. \quad (4.53)$$

The angular-diameter distance is then given as

$$D_A(z) = \frac{1}{1+z} f_K[x(z)], \quad (4.54)$$

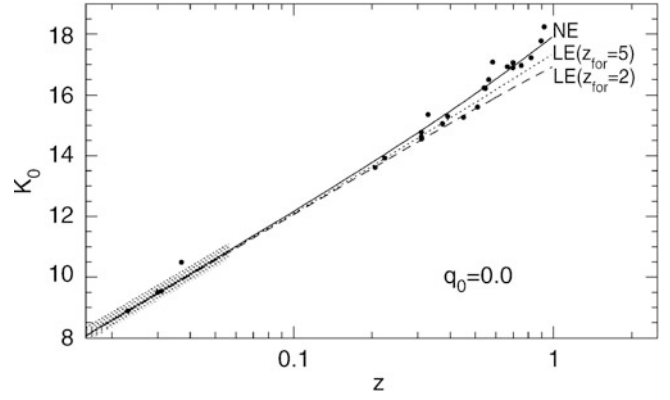


Fig. 4.12 A modern Hubble diagram: for several clusters of galaxies, the K-band magnitude of the brightest cluster galaxy is plotted versus the escape velocity, measured as redshift $z = \Delta\lambda/\lambda$ (symbols). If these galaxies all had the same luminosity, the apparent magnitude would be a measure of distance. For low redshifts, the curves follow the linear Hubble law (4.9), with $z \approx v/c$, whereas for higher redshifts modifications to this law are necessary. The solid curve corresponds to a constant galaxy luminosity at all redshifts, whereas the two other curves take evolutionary effects of the luminosity into account according to models of population synthesis (Sect. 3.5). Two different epochs of star formation were assumed for these galaxies. The diagram is based on a cosmological model with a deceleration parameter of $q_0 = 0$ [see (4.35)]. Source: A. Aragon-Salamanca et al. 1998, *The K-band Hubble diagram for the brightest cluster galaxies: a test of hierarchical galaxy formation models*, MNRAS 297, 427, p. 429, Fig. 1. Reproduced by permission of Oxford University Press on behalf of the Royal Astronomical Society

and thus can be computed for all redshifts and cosmological parameters by (in general numerical) integration of (4.53). The luminosity distance then follows from (4.52). The angular-diameter distance of a source at redshift z_2 , as measured by an observer at redshift $z_1 < z_2$, reads

$$D_A(z_1, z_2) = \frac{1}{1+z_2} f_K[x(z_2) - x(z_1)]. \quad (4.55)$$

This is the distance that is required in equations of gravitational lens theory for D_{ds} . In particular, $D_A(z_1, z_2) \neq D_A(z_2) - D_A(z_1)$.

Sometimes, the look-back time is used as another quantity characterizing the ‘distance’ of a source. It is defined as the time the light traveled from a source at redshift z to us, and can be calculated in analogy to (4.36), with the lower and upper limit of integration being $a = (1+z)^{-1}$ and 1, respectively.

4.3.4 Special case: The Einstein–de Sitter model

As a final note in this section, we will briefly examine one particular cosmological model more closely, namely the model with $\Omega_\Lambda = 0$ and vanishing curvature, $K = 0$, and hence $\Omega_m = 1$. We disregard the radiation component, which

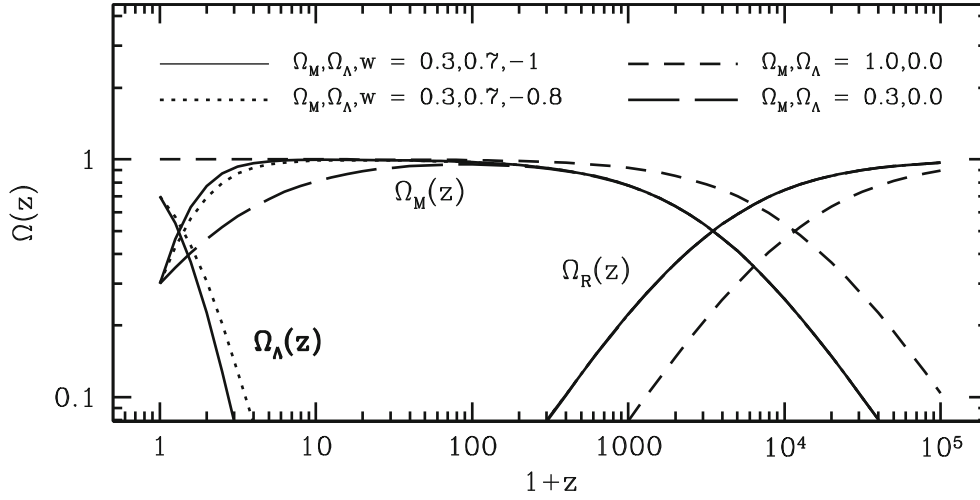


Fig. 4.13 The ratio of the density of the different components in the universe to the critical density $\rho_{\text{cr}}(z) = 3H^2(z)/(8\pi G)$, as a function of redshift, for four different cosmological models: the *solid curves* correspond to the model which is presumably the one we live in, the *short-dashed curves* correspond to an Einstein–de Sitter model, and the *long-dashed curves* show a low density universe without dark energy. Finally, the *dotted curve* corresponds to a case with a different model

for the dark energy. In all cases, radiation dominates the energy density of the universe at early times, i.e., at high redshifts, whereas for z below $\sim 10^4$ the universe becomes matter dominated. Only at redshift below ~ 2 does dark energy contribute significantly to the energy budget, but then quickly starts to dominate. Source: M. Voit 2004, *Tracing cosmic evolution with clusters of galaxies*, astro-ph/0410173, Fig. 2. Reproduced with permission of the author

contributes to the expansion only at very early times and thus for very small a . For a long time, this Einstein–de Sitter (EdS) model was the preferred model among cosmologists because inflation (see Sect. 4.5.3) predicts $K = 0$ and because a finite value for the cosmological constant was considered ‘unnatural’. In fact, as late as the mid-1990s, this model was termed the ‘standard model’. In the meantime we have learned that $\Lambda \neq 0$; thus we are not living in an EdS universe. But there is at least one good reason to examine this model a bit more, since the expansion equations become much simpler for these parameters and we can formulate simple explicit expressions for the quantities introduced above. These then yield estimates which for other model parameter values are only possible by means of numerical integration.

The resulting expansion equation $\dot{a} = H_0 a^{-1/2}$ is easily solved by making the ansatz $a = (Ct)^\beta$ which, when inserted into the equation, yields the solution

$$a(t) = \left(\frac{3 H_0 t}{2} \right)^{2/3} = \left(\frac{t}{t_0} \right)^{2/3}. \quad (4.56)$$

Setting $a = 1$, we obtain the age of the Universe, $t_0 = 2/(3H_0)$. The same result also follows immediately from (4.36) if the parameters of an EdS model are inserted there. Using $H_0 \approx 70 \text{ km s}^{-1} \text{ Mpc}^{-1}$ results in an age of about 10 Gyr, which is slightly too low to be compatible with the age of the oldest star clusters. The angular-diameter distance (4.49) in an EdS universe is obtained by considering the Mattig relation (4.41) for the case $\Omega_m = 1$:

$$D_A(z) = \frac{2c}{H_0} \frac{1}{(1+z)} \left(1 - \frac{1}{\sqrt{1+z}} \right),$$

$$D_L(z) = \frac{2c}{H_0} (1+z) \left(1 - \frac{1}{\sqrt{1+z}} \right), \quad (4.57)$$

where we used (4.52) to obtain the second relation from the first.

4.3.5 Summary

We shall summarize the most important points of the two preceding lengthy sections:

- Observations are compatible with the fact that the Universe around us is isotropic and homogeneous on large scales. The cosmological principle postulates this homogeneity and isotropy of the Universe.
- General Relativity allows homogeneous and isotropic world models, the Friedmann–Lemaître models. In the language of GR, the cosmological principle reads as follows: “A family of solutions of Einstein’s field equations exists such that a set of comoving observers see the same history of the universe; for each of them, the universe appears isotropic.”
- The *shape* of these Friedmann–Lemaître world models is characterized by the density parameter Ω_m and by the cosmological constant Ω_Λ , the *size* by the Hubble constant H_0 . The cosmological parameters determine the expansion rate of the universe as a function of time.

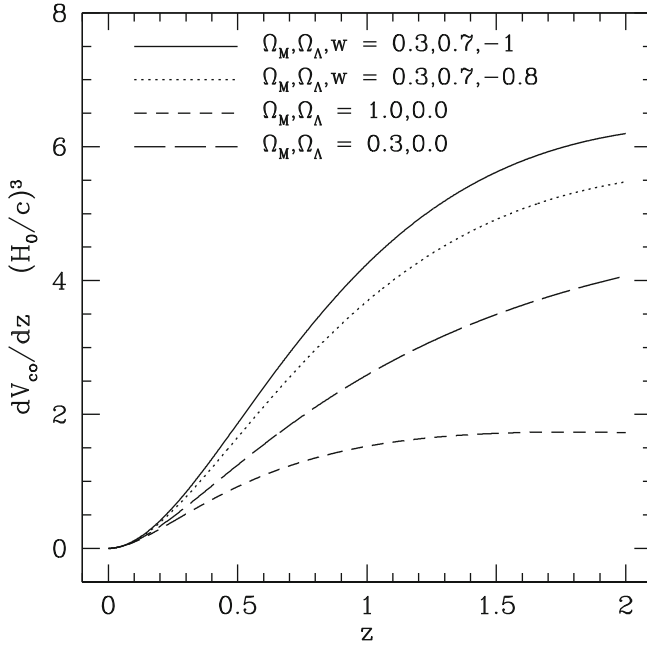


Fig. 4.14 The comoving volume of spherical shells per unit redshift interval, scaled by $(c/H_0)^3$, for the same cosmological models as shown in Fig. 4.13. Obviously, the transformation of a redshift interval into a volume element is a strong function of the density parameters; the volume is smallest for the Einstein–de Sitter model, and largest for the flat, low-density universe. Source: M. Voit 2004, *Tracing cosmic evolution with clusters of galaxies*, astro-ph/0410173, Fig. 3. Reproduced with permission of the author

- The scale factor $a(t)$ of the universe is a monotonically increasing function from the beginning of the universe until now; at earlier times the universe was smaller, denser, and hotter. There must have been an instant when $a \rightarrow 0$, which is called the Big Bang. The future of the expansion depends on Ω_m and Ω_Λ .
- The expansion of the universe causes a redshift of photons. The more distant a source is from us, the more its photons are redshifted.
- The relative contribution of radiation, matter and vacuum energy density changes over cosmic time, with radiation dominating in the first phase of the universe, changing to a matter-dominated universe, to become dark-energy dominated at late times, provided $\Omega_\Lambda > 0$ (see Fig. 4.13).
- ‘Distance’ in cosmology does not have a unique meaning. Depending on whether one relates fluxes to luminosity, or length scales with angular sizes, one needs to use different definitions of distances. The distance-redshift relations depend on the values of the cosmological parameters—they all scale with the Hubble length c/H_0 , and depend on the density parameters. Accordingly, the volume of a spherical shell with given thickness in redshift also depends on the density parameters—which is important when source counts are used to infer number density of sources (see Fig. 4.14).

At <http://www.astro.ucla.edu/~wright/CosmoCalc.html> the reader can find an online calculator for distances, ages, lookback-times etc. as a function of redshift, for different cosmological parameters.

4.4 Thermal history of the Universe

Since $T \propto (1+z)$ our Universe was hotter at earlier times. For example, at a redshift of $z = 1100$ the temperature (of the CMB) was about $T \sim 3000$ K. And at an even higher redshift, $z = 10^9$, it was $T \sim 3 \times 10^9$ K, hotter than in a stellar interior. Thus we might expect energetic processes like nuclear fusion to have taken place in the early Universe.

In this section we shall describe the essential processes in the early universe. To do so we will assume that the laws of physics have not changed over time. This assumption is by no means trivial—we have no guarantee whatsoever that the cross sections in nuclear physics were the same 13 billion years ago as they are today. But if they have changed in the course of time the only chance of detecting this is through cosmology. Based on this assumption of time-invariant physical laws, we will study the consequences of the Big Bang model developed in the previous section and then compare them with observations. Only this comparison can serve as a test of the success of the model. A few comments should serve as preparation for the discussion in this section.

1. Temperature and energy may be converted into each other since $k_B T$ has the dimension of energy. We use the electron volt (eV) to measure temperatures and energies, with the conversion $1 \text{ eV} = 1.1605 \times 10^4 k_B \text{ K}$.
2. Elementary particle physics is very well understood for energies below ~ 100 GeV. For much higher energies our understanding of physics is a lot less certain. Therefore, we will begin the consideration of the thermal history of the cosmos at energies well below this scale.
3. Statistical physics and thermodynamics of elementary particles are described by quantum mechanics. A distinction has to be made between *bosons*, which are particles of integer spin (like the photon), and *fermions*, particles of half-integer spin (like, for instance, electrons, protons, neutrinos, and their anti-particles).
4. If particles are in thermodynamical and chemical equilibrium, their number density and their energy distribution are specified solely by the temperature—e.g., the Planck distribution (A.13), and thus the energy density of the radiation (4.26), is a function of T only.

The necessary condition for establishing chemical equilibrium is the possibility for particles to be created and destroyed, such as in e^+e^- -pair production and annihilation.

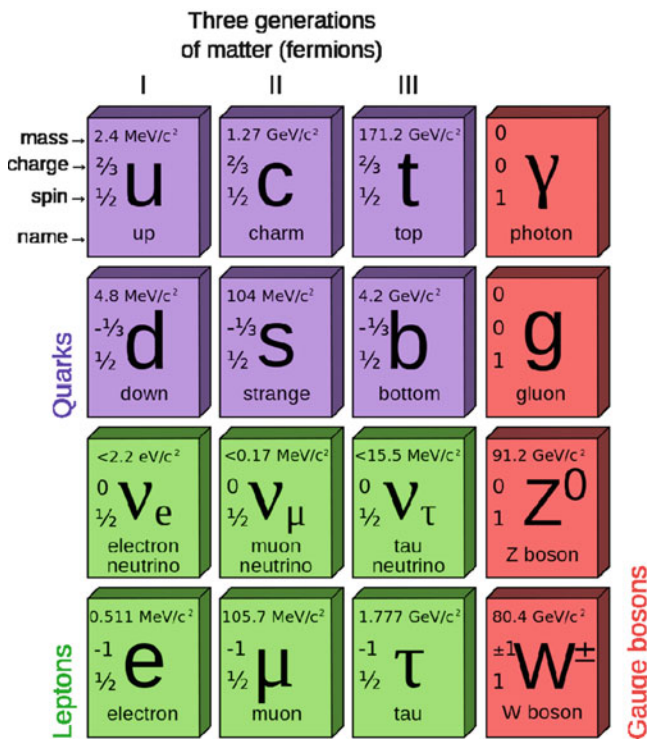


Fig. 4.15 The particles in the Standard Model: The six quarks (violet) and six leptons (green) are organized in three families; the four gauge bosons are shown in red. The numbers in each box indicate particle mass, charge (in units of the elementary charge) and spin. All particles have an antiparticle, except the photon and the Z-boson, which are their own antiparticles. Not shown in the diagram is the recently found Higgs particle. Source: Wikipedia

4.4.1 The Standard Model of particle physics

Before discussing the events in the early history of the Universe in more detail, it is useful to briefly summarize what we know about particle physics. Since about the 1970s, the Standard Model has been in place; it describes the elementary particles and their interactions—except for gravity.

Particle contents. According to this model, matter is composed of fermions, particles with half-integer spin, which obey the Pauli exclusion principle. The fermions are further divided into leptons, such as the electron and the electron neutrino, and quarks, such as the up and down quark. Figure 4.15 provides an overview on the particles of the Standard Model, together with information on their mass, charge and spin. All of the particles have anti-particles; for example, the positron is the anti-particle of the electron, its charge is minus the electron's charge; some of the particles are their own anti-particle, such as the photon. The quarks, particles with the strange property that their charge is not a multiple of the elementary charge, but thirds of it, form bound states, such as the proton and the neutron, being composed of three quarks each. In fact, according to the Standard Model, quarks do

not occur isolated in nature, but are only found in compound systems of hadrons, such as the nucleons, or mesons, such as the pions. According to the model, the former consist of three quarks, the latter of a quark-antiquark system. Protons and neutrons are composed of up and down quarks, the lightest quarks. The electron, the electron neutrino, and the up and down quarks form the so-called first family of particles (see Fig. 4.15).

Except for the electron, there are two more charged leptons, the muon and the tau, which were discovered in 1936 and 1975, respectively. Both of these leptons are much heavier than the electron, and they are unstable: the muon decays into an electron and two neutrinos, whereas the tau can either decay into a muon or an electron, again accompanied with two neutrinos. However, these two charged leptons show properties very similar to those of the electron. For both of them, there is an associated neutrino, the μ -neutrino (ν_μ) and the τ -neutrino (ν_τ). Neutrinos are much more difficult to detect than the charged leptons, since they only interact weakly with matter. Therefore, they were directly detected only in 1956 (ν_e), 1962 (ν_μ) and 2000 (ν_τ)—note that the discovery of the tau-neutrino occurred well after the Standard Model had been well established and presents one of its successes.

Particle accelerators with ever increasing energies produced heavier particles. Among them were also particles which could not be described as composite particles consisting of up and down quarks only, but their understanding implied the presence of additional quarks. By 1970, the strange and charm quarks were thereby indirectly discovered. Together with the muon and its neutrino, these two new quarks form the second family of elementary particles. With the discovery of the tau, two more quarks were predicted, to form the third family—the bottom and top quark were indeed discovered in 1977 and 1995, again as bound states forming heavier compound particles.

Interactions; gauge bosons. According to the Standard Model, interactions between particles occur through the exchange of bosons. The carrier of the electromagnetic force is the photon. The exchange particles for the strong force between quarks is the gluon. Like the photon, it is electrically neutral, but unlike the photon, it carries a new property called color. As for the quarks, an isolated gluon has not been observed yet; nevertheless, its existence was indirectly verified in particle decays in 1979. The strong interaction between quarks transmitted by gluons is described by the theory of Quantum Chromodynamics (QCD), which is the strong interaction part of the Standard Model.

All leptons are subject to weak interactions; the Standard Model postulates the existence of two exchange bosons, the charged W-boson and the electrically neutral Z-boson. Their discovery had to await sufficiently powerful accelerators, but

both were finally found in 1983, a beautiful and impressive confirmation of the Standard Model. The Standard Model predicts that electromagnetic and weak interactions are unified to the electroweak interaction. However, at low energies these two interactions appear to be quite different. The explanation for this difference is that the W- and Z-boson are very massive, whereas the photon is massless. Thus, at energy scales below the Z-boson mass, weak interactions are considerably weaker than electromagnetic ones.

The Higgs mechanism. According to the Standard Model as outlined so far, all particles are intrinsically massless. Obviously, this is not the case; for example, the electron, the muon and the tau have a finite rest mass. One finds that the quarks have a finite rest mass as well. As an aside, we note that the mass of a nucleon is much higher than the sum of the masses of its three constituent quarks; most of the nucleon mass stems from the strong interactions transmitted by the gluons.

A mechanism for particles to obtain a finite rest mass was proposed in the 1960s, and this so-called Higgs-mechanism for symmetry breaking has been widely accepted and became part of the Standard Model. It is responsible for the large masses of the W and Z bosons, and thus for the different appearance of electroweak interactions as weak and electromagnetic ones at low energies. This Higgs mechanism implies the existence of an additional particle, called the Higgs particle. The search for this Higgs particle was one of the main drivers for building the most complex machine ever made by mankind—the Large Hadron Collider at CERN. It can generate sufficiently high energies for the Higgs particle to be generated and discovered. Indeed, in the summer of 2013, scientists from two different collaborations announced the discovery of a new elementary particle, which after a short period was verified as being the long-sought Higgs particle—a spectacular success! With that, the final missing piece of the Standard Model was found. The Nobel Prize in physics 2013 for F. Englert and P. Higgs for the theoretical development of this mechanism acknowledges also the importance of this discovery.

4.4.2 Expansion in the radiation-dominated phase

As mentioned above (4.30), the energy density of radiation dominates in the early universe, at redshifts $z \gg z_{\text{eq}}$ where

$$z_{\text{eq}} = a_{\text{eq}}^{-1} - 1 \approx 23\,900 \, \Omega_{\text{m}} h^2. \quad (4.58)$$

The radiation density behaves like $\rho_r \propto T^4$, where the constant of proportionality depends on the number of species

of relativistic particles (these are the ones for which $k_B T \gg mc^2$). Since $T \propto 1/a$ and thus $\rho_r \propto a^{-4}$, radiation then dominates in the expansion equation (4.18). The latter can be solved by a power law, $a(t) \propto t^\beta$, which after insertion into the expansion equation yields $\beta = 1/2$ and thus

$$\boxed{a \propto t^{1/2}, \quad t = \sqrt{\frac{3}{32\pi G\rho}}, \quad t \propto T^{-2} \text{ in radiation-dominated phase}}, \quad (4.59)$$

where the constant of proportionality depends again on the number of relativistic particle species. Since the latter is known from particle physics, assuming thermodynamical equilibrium, the time dependence of the early expansion is uniquely specified by (4.59). This is reasonable because for early times neither the curvature term nor the cosmological constant contribute significantly to the expansion dynamics.

4.4.3 Decoupling of neutrinos

We start our consideration of the universe at a temperature of $T \approx 10^{12}$ K which corresponds to ~ 100 MeV. This energy can be compared to the rest mass of various particles:

$$\begin{aligned} \text{proton, } m_p &= 938.3 \text{ MeV}/c^2, \\ \text{neutron, } m_n &= 939.6 \text{ MeV}/c^2, \\ \text{electron, } m_e &= 511 \text{ keV}/c^2, \\ \text{muon, } m_\mu &= 140 \text{ MeV}/c^2. \end{aligned}$$

Protons and neutrons (i.e., the baryons) are too heavy to be produced at the temperature considered. Thus all baryons that exist today must have been present already at this early time. Also, the production of muon pairs, according to the reaction $\gamma + \gamma \rightarrow \mu^+ + \mu^-$, is not efficient because the temperature, and thus the typical photon energy, is not sufficiently high. Hence, at the temperature considered the following relativistic particle species are present: electrons and positrons, photons and neutrinos. These species contribute to the radiation density ρ_r . The mass of the neutrinos is not accurately known, though we recently learned that they have a small but finite rest mass. As will be explained in Sect. 8.7, cosmology allows us to obtain a very strict limit on the neutrino mass, which is currently below 1 eV. For the purpose of this discussion they may thus be considered as massless.

In addition to relativistic particles, non-relativistic particles also exist. These are the protons and neutrons, and probably also the constituents of dark matter. We assume that the latter consists of weakly interacting massive particles

(WIMPs), with rest mass larger than ~ 100 GeV because up to these energies no WIMP candidates have been found in terrestrial particle accelerator laboratories. With this assumption, WIMPs are non-relativistic at the energies considered. Thus, like the baryons, they virtually do not contribute to the energy density in the early universe.

Apart from the WIMPs, all the aforementioned particle species are in equilibrium, e.g., by the following reactions:

$e^\pm + \gamma \leftrightarrow e^\pm + \gamma$: Compton scattering,
 $e^+ + e^- \leftrightarrow \gamma + \gamma$: pair-production and annihilation,
 $\nu + \bar{\nu} \leftrightarrow e^+ + e^-$: neutrino-antineutrino-scattering,
 $\nu + e^\pm \leftrightarrow \nu + e^\pm$: neutrino-electron scattering,
 $e^\pm + p \leftrightarrow e^\pm + p + \gamma$: Bremsstrahlung.

Reactions involving baryons will be discussed later. The energy density at this epoch is⁸

$$\rho = \rho_r = 10.75 \frac{\pi^2}{30} \frac{(k_B T)^4}{(\hbar c)^3}, \quad (4.60)$$

which yields—see (4.59)—

$$t \approx 0.3 \text{ s} \left(\frac{T}{1 \text{ MeV}} \right)^{-2}. \quad (4.61)$$

Hence, about one second after the Big Bang the temperature of the Universe was about 10^{10} K. For the particles to maintain equilibrium, the reactions above have to occur at a sufficient rate. The equilibrium state, specified by the temperature, continuously changes due to the expansion of the Universe, so that the particle distribution needs to continually adjust to this changing equilibrium. This is possible only if the mean time between two reactions is much shorter than the time-scale on which equilibrium conditions change. The latter is given by the expansion. This means that the reaction rates (the number of reactions per particle per unit time) must be larger than the cosmic expansion rate $H(t)$ in order for the particles to maintain equilibrium.

The reaction rates Γ are proportional to the product of the number density n of the reaction partner particles and the cross section σ of the corresponding reaction. Both decrease with time: the number density decreases as $n \propto a^{-3} \propto t^{-3/2}$ because of the expansion. Furthermore, the cross sections for weak interaction, which is responsible for the reactions involving neutrinos, depend on energy, approximately as

$\sigma \propto E^2 \propto T^2 \propto a^{-2}$. Together this yields $\Gamma \propto n\sigma \propto a^{-5} \propto t^{-5/2}$, whereas the expansion rate decreases only as $H \propto t^{-1}$. At sufficiently early times, the reaction rates were larger than the expansion rate, and thus particles remained in equilibrium. Later, however, the reactions no longer took place fast enough to maintain equilibrium. The time or temperature, respectively, of this transition can be calculated from the cross section of weak interaction,

$$\frac{\Gamma}{H} \approx \left(\frac{T}{1.6 \times 10^{10} \text{ K}} \right)^3,$$

so that for $T \lesssim 10^{10}$ K neutrinos are no longer in equilibrium with the other particles. This process of decoupling from the other particles is also called *freeze-out*; neutrinos freeze out at $T \sim 10^{10}$ K. At the time of freeze-out, they had a thermal distribution with the same temperature as the other particle species which stayed in mutual equilibrium. From this time on neutrinos propagate without further interactions, and so have kept their thermal distribution up to the present day, with a temperature decreasing as $T \propto 1/a$. This consideration predicts that these neutrinos, which decoupled from the rest of the matter about one second after the Big Bang, are still around in the Universe today. They have a number density of 113 cm^{-3} per neutrino family and are at a temperature of 1.9 K (this value will be explained in more detail below). However, these very low energy neutrinos are currently undetectable because of their extremely low cross section.

The expansion behavior is unaffected by the neutrino freeze-out and continues to proceed according to (4.61).

4.4.4 Pair annihilation

At temperatures smaller than $\sim 5 \times 10^9$ K, or $k_B T \sim 500$ keV, electron-positron pairs can no longer be produced efficiently since the number density of photons with energies above the pair production threshold of 511 keV is becoming too small. However, the annihilation $e^+ + e^- \rightarrow \gamma + \gamma$ continues to proceed and, due to its large cross section, the density of e^+e^- -pairs decreases rapidly.

Pair annihilation injects additional energy into the photon gas, originally present as kinetic and rest mass energy of the e^+e^- pairs. This changes the energy distribution of photons, which continues to be a Planck distribution but now with a modified temperature relative to that it would have had without annihilation. The neutrinos, already decoupled at this time, do not benefit from this additional energy. This means that after the annihilation the photon temperature exceeds that of the neutrinos. From the thermodynamics of this process, the change in photon temperature is computed as

⁸Compare this energy density with that of a blackbody photon distribution; they are the same except for the prefactor. This prefactor is determined by the number of bosonic and fermionic particle species which are relativistic at temperature T .

$$\begin{aligned}
& (aT)(\text{after annihilation}) \\
&= \left(\frac{11}{4}\right)^{1/3} (aT)(\text{before annihilation}) \\
&= \left(\frac{11}{4}\right)^{1/3} (aT_\nu)
\end{aligned} \quad (4.62)$$

This temperature ratio is preserved afterwards, so that neutrinos have a temperature lower than that of the photons by $(11/4)^{1/3} \sim 1.4$ —until the present epoch. This result has already been mentioned and taken into account in the estimate of $\rho_{r,0}$ in (4.28); we find $\rho_{r,0} = 1.68\rho_{\text{CMB},0}$.

The factor 1.68 in the foregoing equation originates from the fact that the energy density of neutrinos is related to that of the photons through

$$\rho_\nu = N_{\text{eff}} \frac{7}{8} \left(\frac{4}{11}\right)^{4/3} \rho_{\text{CMB}}, \quad (4.63)$$

where N_{eff} is the number of neutrino families, the factor $(7/8)$ is derived from quantum statistics and accounts for the fact that neutrinos are fermions, whereas photons are bosons, and the factor $(4/11)^{4/3}$ stem from the different temperatures of neutrinos and photons after pair annihilation. With three neutrino families, one has $N_{\text{eff}} = 3$, according to the consideration above. However, since the temperature at which neutrino freeze-out happens, is very close to that of pair annihilation, the treatment of both processes as done above is slightly simplistic. We have assumed that the neutrinos are fully decoupled before pair annihilation sets in; an accurate treatment accounts for the fact that these processes are not fully decoupled. Such an accurate treatment confirms the relation (4.63), but with a slightly different value of $N_{\text{eff}} = 3.046$.

After pair annihilation, the expansion law

$$t = 0.55 \text{ s} \left(\frac{T}{1 \text{ MeV}}\right)^{-2} \quad (4.64)$$

applies. This means that, as a result of annihilation, the constant in this relation changes compared to (4.61) because the number of relativistic particles species has decreased. Furthermore, the ratio η of the baryon-to-photon number density remains constant after pair annihilation.⁹ The former is characterized by the density parameter $\Omega_b = \rho_{b,0}/\rho_{\text{cr}}$ in baryons (today), and the latter is determined by T_0 :

$$\eta := \left(\frac{n_b}{n_\gamma}\right) = 2.74 \times 10^{-8} (\Omega_b h^2). \quad (4.65)$$

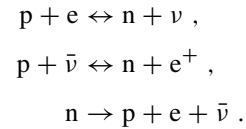
As we will see in a moment, in our Universe $\Omega_b h^2 \approx 0.02$, which means that for every baryon there are about two billion photons. Before pair annihilation there were about as many electrons and positrons as there were photons. After annihilation *nearly* all electrons were converted into photons—but not entirely because there was a very small

excess of electrons over positrons to compensate for the positive electrical charge density of the protons. Therefore, the number density of electrons that survive the pair annihilation is exactly the same as the number density of protons, for the Universe to remain electrically neutral. Thus, the ratio of electrons to photons is also given by η , or more precisely by about 0.8η , since η includes both protons and neutrons.

4.4.5 Primordial nucleosynthesis

Protons and neutrons can fuse to form atomic nuclei if the temperature and density of the plasma are sufficiently high. In the interior of stars, these conditions for nuclear fusion are provided. The high temperatures in the early phases of the Universe suggest that atomic nuclei may also have formed then. As we will discuss below, in the first few minutes after the Big Bang some of the lightest atomic nuclei were formed. The quantitative discussion of this primordial nucleosynthesis (Big Bang nucleosynthesis, BBN) will explain observation (4) of Sect. 4.1.1.

Proton-to-neutron abundance ratio. As already discussed, the baryons (or nucleons) do not play any role in the expansion dynamics in the early universe because of their low density. The most important reactions through which they maintain chemical equilibrium with the rest of the particles are



The latter is the decay of free neutrons, with a time-scale for the decay of $\tau_n = 881 \text{ s}$. The first two reactions maintain the equilibrium proton-to-neutron ratio as long as the corresponding reaction rates are large compared to the expansion rate. The equilibrium distribution is specified by the Boltzmann factor,

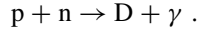
$$\frac{n_n}{n_p} = \exp\left(-\frac{\Delta m c^2}{k_B T}\right), \quad (4.66)$$

where $\Delta m = m_n - m_p = 1.293 \text{ MeV}/c^2$ is the mass difference between neutrons and protons. Hence, neutrons are slightly heavier than protons; otherwise the neutron decay would not be possible. After neutrino freeze-out equilibrium reactions become rare because the above reactions are based on weak interactions, the same as those that kept the neutrinos in chemical equilibrium. At the time of neutrino decoupling, we have $n_n/n_p \approx 1/3$. After this, protons and neutrons are no longer in equilibrium, and their ratio is no longer described by (4.66). Instead, it changes only by the decay of free neutrons on the time-scale τ_n . To have neutrons

⁹The total number of photons emitted during stellar evolution is negligible compared to the number of CMB photons.

survive at all until the present day, they must quickly become bound in atomic nuclei.

Deuterium formation. The simplest compound nucleus is that of deuterium (D), consisting of a proton and a neutron and formed in the reaction



The binding energy of D is $E_b = 2.225 \text{ MeV}$. This energy is only slightly larger than $m_e c^2$ and Δm —all these energies are comparable. The formation of deuterium is based on strong interactions and therefore occurs very efficiently. However, at the time of neutrino decoupling and pair annihilation, T is not much smaller than E_b . This has an important consequence: because photons are so much more abundant than baryons, a sufficient number of highly energetic photons, with $E_\gamma \geq E_b$, exist in the Wien tail of the Planck distribution to instantly destroy newly formed D by photo-dissociation. Only when the temperature has decreased considerably, $k_B T \ll E_b$, can the deuterium abundance become appreciable. With the corresponding balance equations we can calculate that the formation rate exceeds the photo-dissociation rate of deuterium at about $T_D \approx 8 \times 10^8 \text{ K}$, corresponding to $t \sim 3 \text{ min}$. Up to then, a fraction of the neutrons has thus decayed, yielding a neutron-proton ratio at T_D of $n_n/n_p \approx 1/7$.

After that time, everything happens very rapidly. Owing to the strong interaction, virtually all neutrons first become bound in D. Once the deuterium density has become appreciable, helium (He^4) forms, which is a nucleus with high binding energy ($\sim 28 \text{ MeV}$) which can therefore not be destroyed by photo-dissociation. Except for a small (but, as we will later see, very important) remaining fraction, all deuterium is quickly transformed into He^4 . For this reason, the dependence of helium formation on the small binding energy of D is known as the ‘bottleneck of nucleosynthesis’.

Helium abundance. The number density of helium nuclei can now be calculated, since virtually all neutrons present are bound in He^4 . First, $n_{\text{He}} = n_n/2$, since every helium nucleus contains two neutrons. Second, the number density of free protons after the formation of helium is $n_H = n_p - n_n$, since He^4 contains an equal number of protons and neutrons. From this, the mass fraction Y of He^4 of the baryon density follows,

$$Y = \frac{4n_{\text{He}}}{4n_{\text{He}} + n_H} = \frac{2n_n}{n_p + n_n} = \frac{2(n_n/n_p)}{1 + (n_n/n_p)} \approx 0.25, \quad (4.67)$$

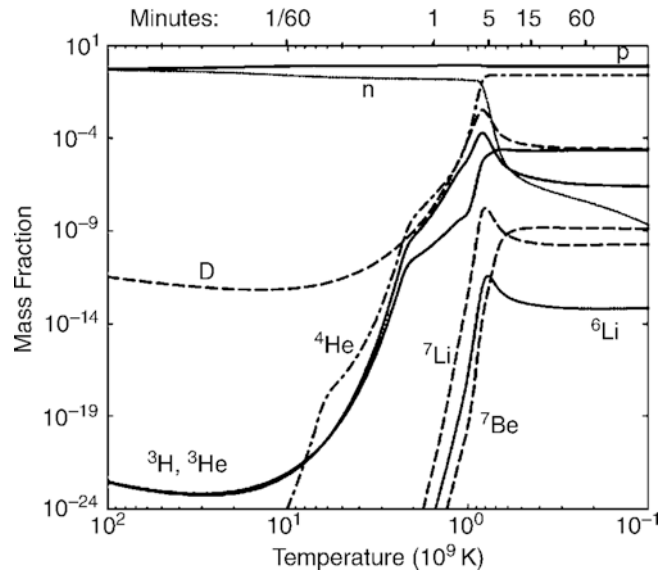


Fig. 4.16 The evolution of abundances of the light elements formed in BBN, as a function of temperature (lower axis) and cosmic time t (upper axis). The decrease in neutron abundance in the first $\sim 3 \text{ min}$ is due to neutron decay. The density of deuterium increases steeply—linked to the steep decrease in neutron density—and reaches a maximum at $t \sim 3 \text{ min}$ because then its density becomes sufficiently large for efficient formation of He^4 to set in. Only a few deuterium nuclei do not find a reaction partner and remain, with a mass fraction of $\sim 10^{-5}$. Only a few other light nuclei are formed in the Big Bang, mainly He^3 and Li^7 . Source: D. Tytler, J.M. O’Meara, N. Suzuki & D. Lubin 2000, *Deuterium and the baryonic density of the universe*, Phys. Rep. 333, 409–432. Reprinted with permission from Elsevier

where in the last step we used the above ratio of $n_n/n_p \approx 1/7$ at T_D . This consideration thus leads to the following conclusion:

About 1/4 of the baryonic mass in the Universe should be in the form of He^4 . This is a robust prediction of Big Bang models, and it is in excellent agreement with observations.

The helium content in the Universe changes later by nuclear fusion in stars, which also forms heavier nuclei (‘metals’), but as derived in problem 2.2, the total amount of helium produced in stars is expected to be smaller by about one order of magnitude compared to that in BBN. Observations of fairly unprocessed material (i.e., that which has a low metal content) reveal that in fact $Y \approx 0.25$. Figure 4.16 shows the result of a quantitative model of BBN where the mass fraction of several species is plotted as a function of time or temperature, respectively.

Dependence of the primordial abundances on the baryon density. At the end of the first 3 min, the composition of the baryonic component of our Universe is about as follows: 25 % of the baryonic mass is bound in helium nuclei, 75 % in hydrogen nuclei (i.e., protons), with traces of D, He^3 and Li^7 . Heavier nuclei cannot form because no stable nucleus of mass number 5 or 8 exists and thus no new, stable nuclei can be formed in collisions of two helium nuclei or of a proton with a helium nucleus. Collisions between three nuclei are far too rare to contribute to nucleosynthesis. The density in He^4 and D depends on the baryon density in the Universe, as can be seen in Fig. 4.17 and through the following considerations:

- The larger the baryon density Ω_b , thus the larger the baryon-to-photon ratio η (4.65), the earlier D can form, i.e., the fewer neutrons have decayed, which then results in a larger n_n/n_p ratio. From this and (4.67) it follows that Y increases with increasing Ω_b .
- A similar argument is valid for the abundance of deuterium: the larger Ω_b is, the higher the baryon density during the conversion of D into He^4 . Thus the conversion will be more efficient and more complete. This means that fewer deuterium nuclei remain without a reaction partner for helium formation. Thus fewer of them are left over in the end, so the fraction of D will be lower.

Baryon content of the Universe. From measurements of the primordial abundances of He^4 and D and their comparison with detailed models of nucleosynthesis in the early Universe, η or Ω_b , respectively, can be determined (see Fig. 4.17). The abundance of deuterium is a particularly sensitive measure for Ω_b . Measurements of the relative strength of the $\text{Ly}\alpha$ lines of H and D, which have slightly different transition frequencies due to the different masses of their nuclei, in QSO absorption lines (see Sect. 5.7) yields $\text{D}/\text{H} \approx 3.4 \times 10^{-5}$. Since the intergalactic gas producing these absorption lines is very metal-poor and thus presumably barely affected by nucleosynthesis in stars, its D/H-ratio should be close to the primordial value. Combining the quoted value of D/H with the model curves shown in Fig. 4.17 we find

$$\boxed{\Omega_b h^2 \approx 0.02} . \quad (4.68)$$

With a Hubble constant of $H_0 \sim 70 \text{ km s}^{-1} \text{ Mpc}^{-1}$, thus $h^2 \approx 1/2$, we have $\Omega_b \approx 0.04$. But since $\Omega_m > 0.1$, this result implies that baryons represent only a small fraction of the matter in the Universe. *The major fraction of matter is non-baryonic dark matter.*

To circumvent the conclusion of a dominant fraction of non-baryonic matter, inhomogeneous models of BBN have

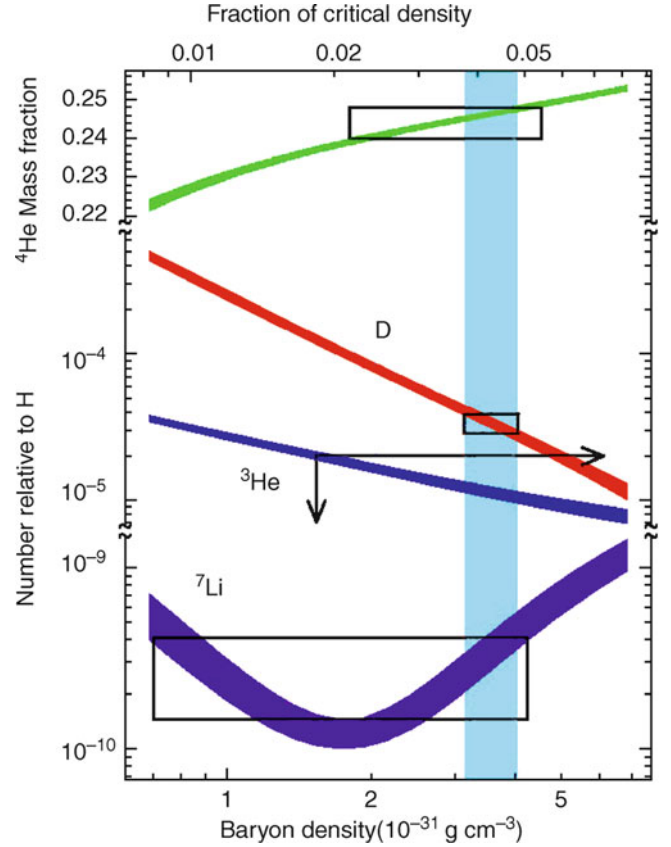


Fig. 4.17 BBN predictions of the primordial abundances of light elements as a function of today's baryon density ($\rho_{b,0}$, lower axis) and the corresponding density parameter Ω_b where $h = 0.65$ was assumed. The vertical extent of the rectangles marks the measured values of the abundances (top: He^4 , center: D, bottom: Li^7). The horizontal extent results from the overlap of these intervals with curves computed from theoretical models. The ranges in Ω_b that are allowed by these three species do overlap, as is indicated by the vertical strip. The deuterium measurements yield the most stringent constraints for Ω_b . Source: D. Tytler, J.M. O'Meara, N. Suzuki & D. Lubin 2000, *Deuterium and the baryonic density of the universe*, Phys. Rep. 333, 409–432. Reprinted with permission from Elsevier

been investigated, but these also yield values for Ω_b which are too low and therefore do not provide a viable alternative.

Dependence of BBN on the number of neutrino flavors.

In the analysis of BBN we implicitly assumed that not more than three (relativistic, i.e., with $m_\nu < 1 \text{ MeV}$) neutrino families exist. If $N_\nu > 3$, the quantitative predictions of BBN will change. In this case, the expansion would occur faster [see (4.59)] because $\rho(T)$ would be larger, leaving less time until the temperature has cooled down to T_D —thus, fewer neutrons would decay and the resulting helium abundance would be higher. Even before 1990, it was concluded from BBN (with relatively large uncertainties, however) that $N_\nu = 3$. In 1990, the value of $N_\nu = 3$ was then confirmed in the laboratory from Z-boson decay.

4.4.6 WIMPs as dark matter particles

There is a wide variety of evidence for the existence of dark matter, from scales of individual galaxies (rotation curves of spirals), clusters (velocity dispersion of galaxies, X-ray temperature, lensing), to cosmological scales, where the baryon density as inferred from BBN is lower than the lower bound on the total matter density. The MACHO experiments described in Sect. 2.5.3 rule out astronomical objects as the dominant contribution to dark matter, at least in the halo of the Milky Way; furthermore, all obvious candidates for astronomical dark matter objects would yield very strong conflicts with observations, for example concerning metallicity. In addition, the fact that the mass density in the Universe is ~ 6 times higher than the baryonic density precludes any ‘normal’ astronomical objects as the main constituent of dark matter. Therefore, the solution of the dark matter issue must likely come from particle physics.

Constraints on the dark matter particle. Since dark matter particles are ‘dark’ they must be electrically neutral in order not to interact electromagnetically. Furthermore, the particle must be stable, or at least have a lifetime much longer than the age of the Universe, so that they are still around today. The only known neutral particles in the Standard Model (see Sect. 4.4.1) are the neutrinos and the neutron. However, the neutron is baryonic, and its density in the early Universe is very well constrained by BBN (see Sect. 4.4.5); furthermore, the free neutron is unstable and thus clearly not a viable dark matter candidate. The neutrinos in principle could be good dark matter candidates if they have a finite mass, since we know they exist, and we actually know their abundance and their temperature, which were determined at their decoupling—see Sect. 4.4.3. But they would be hot dark matter, and as such lead to a large-scale structure in the Universe that would be very different from the one we observe, as will be explained in more detail in Sect. 7.4.1. In particular, they would be too ‘hot’ to cluster on scales of galaxies, with their thermal velocity exceeding that of the escape velocity from galaxy halos. We thus conclude that none of the known particles is a viable dark matter candidate.

Physics beyond the Standard Model. This Standard Model of particle physics has proved extremely successful in describing subatomic physics, as discussed in Sect. 4.4.1. Predictions of low-energy electromagnetic phenomena agree with laboratory measurements to better than one part in a billion, and for electro-weak interactions, the agreement is better than 10^{-3} . Because of its strengths and of non-linearities, strong interactions are far more difficult to describe quantitatively from first principles, and thus the strong interaction sector of the standard model—quantum

chromodynamics (QCD)—is less accurately tested than the weak and electromagnetic part.

Despite its successes, the standard model is known to be incomplete, and in at least one aspect, it directly conflicts with observations: According to the standard model, neutrinos should be massless. However, the Solar neutrino problem and its solution has shown this to be not the case: The (electron) neutrinos generated through nuclear fusion in the center of the Sun can escape, due to their small interaction cross section. These Solar neutrinos can be detected in (big!) terrestrial detectors.¹⁰ However, the measured rate of electron neutrinos from the Sun is only half as large as expected from Solar models. This *Solar neutrino problem* kept physicists and astrophysicists busy for decades. Its solution consists of a purely quantum-mechanical process, that of neutrino oscillations. It is possible that during its propagation, an electron neutrino transforms into a muon or tau neutrino, and back again. The existence of such oscillations was speculated for a long time, and provides a possible explanation for the missing rate of Solar electron neutrinos. Indeed, in 2001 the Sudbury Neutrino Observatory showed that neutrinos of all three flavors are received from the Sun, and that the sum of the rates of these neutrinos is compatible with the predicted rate from Solar models. In the meantime, these neutrino oscillations have also been observed in terrestrial experiments with neutrino beams.

Whereas neutrino oscillations are therefore well established today, they are in conflict with the Standard Model, according to which neutrinos have zero rest mass. From Special Relativity one can easily show that massless particles can not change their ‘identity’ while propagating through space. The existence of neutrino oscillations necessarily requires that neutrinos have a finite rest mass. Indeed, the oscillation experiments were able to constrain these masses, since they determine the length-scale over which the flavor of neutrinos changes—more precisely, it depends on the difference of their squared mass m_i^2 . One finds that $m_2^2 - m_1^2 = (7.6 \pm 0.2) \times 10^{-5} \text{ eV}^2$, and $|m_3^2 - m_2^2| \approx |m_3^2 - m_1^2| = (2.4 \pm 0.2) \times 10^{-3} \text{ eV}^2$. These squared-mass differences thus do not provide us with an absolute mass scale of neutrinos, but their mass is non-zero. That means that neutrinos contribute to the cosmic matter density today, giving a contribution of

$$\Omega_\nu h^2 = \frac{\sum m_{\nu i}}{91.5 \text{ eV}}, \quad (4.69)$$

which depends only on the sum of the three neutrino masses—since the number density of neutrinos is known

¹⁰For their research in the field of Solar neutrinos, Raymond Davis and Masatoshi Koshiba were awarded with one half of the Nobel Prize in Physics in 2002. The other half was awarded to Riccardo Giacconi for his pioneering work in the field of X-ray astronomy.

from the thermal history after the Big Bang. If the neutrino masses take the lowest values allowed by the squared-mass differences given above, this contribution is about 0.1%. We will see in Chap. 8 that observations of the large-scale structure in the Universe show that neutrinos cannot contribute a substantial fraction to the matter density. Indeed, these observations yield a constraint of $\sum m_{\nu i} \lesssim 1$ eV, and thus the upper bound on neutrino masses from cosmology are much stricter than those obtained from laboratory experiments. For the electron neutrino, an upper limit on its mass was determined from decay experiments of tritium, yielding $m_{\nu_e} \lesssim 2$ eV, which together with the results from neutrino oscillations implies a maximum density of $\Omega_\nu < 0.12$.

Physical motivation for WIMPs. Hence, the Standard Model needs an extension which allows the existence of a finite neutrino mass. In addition, there are other issues with the Standard Model—it is “technically unnatural” since the energy scale of the Higgs boson, ~ 125 GeV, which is also comparable to the electro-weak mass scale, i.e., the masses of the W and Z bosons, is so much smaller than the Planck mass,¹¹ and it can also not explain why there are more baryons than anti-baryons in the current Universe. The former of these problems is called the gauge hierarchy problem; in order to solve it, one needs some new physics at an energy scale of ~ 100 GeV. There are several models, extending the Standard Model, which introduce new physics at this scale. Arguably, the most promising of those is supersymmetry.

Then suppose that in the extended model, there exists a electrically neutral particle X which is stable, has a mass of order the energy scale of the model, i.e., somewhere between 100 GeV and 10 TeV, and interacts only weakly.¹² Such Weakly Interacting Massive Particles (WIMPs) are the most promising dark matter candidates—because, if such a particle exists, it would have the right cosmic density to account for the dark matter.

¹¹From the fundamental constants G , c and \hbar , one can form a unique combination with the dimension of a mass, $m_{\text{Pl}} = \sqrt{\hbar c/G} \sim 10^{19}$ GeV, called the Planck mass. This is the mass scale where one expects that General Relativity ceases to be valid and that it has to be generalized to a quantum theory of gravity. Up to now, no plausible model for such a quantum gravity has been found.

¹²One might be surprised about the assumption that a particle of such high mass should be stable—given that there are only very few particles known to be stable, and they all have very small mass—the heaviest one being the proton. The Standard Model predicts that the baryon number is a conserved quantity, i.e., one cannot change the net number of baryons. For example, in creating a proton–antiproton pair, the net baryon number is changed by $+1 - 1 = 0$; in the decay of the free neutron, baryon number is conserved as well. Since the proton is the lightest baryon, there is no particle into which it can decay without violating baryon conservation—that’s why we believe the proton is stable. If such a conserved quantity exists in the extended model of elementary particles (for example, in supersymmetry there is a so-called R-parity), then the lightest of the particles which ‘carries’ this quantity must be stable as well.

At first sight, it may be difficult to see how one can estimate the cosmic mass density of a particle whose existence and properties are as yet unknown, but indeed we can. For that, recall how we obtained the abundance of neutrinos in the Universe. Above a certain temperature, they were in thermodynamic equilibrium with the rest of the matter in the Universe, but when their interaction rate became too slow, they dropped out of equilibrium with the rest of the matter in the Universe, and kept their comoving number density from then on.

Now, let’s assume the WIMP particle X exists. At sufficiently early times, it was in thermodynamic equilibrium. Since it is weakly interacting by assumption, we have a good idea about its cross section, and thus conclude that it stays in equilibrium during the phase when the temperature of the Universe drops below $T \sim m_X c^2 = \mathcal{O}(1 \text{ TeV})$, i.e., when the particles become non-relativistic. Once this happens, the equilibrium number density is determined by the Boltzmann factor,

$$n_{X,\text{eq}} \propto (m_X T)^{3/2} e^{-m_X/T}$$

and thus starts to decrease rapidly with decreasing T . At $T \approx 0.05 m_X$, the interaction rate of X becomes too small to keep them in equilibrium with the other particles present, they freeze out, and from then on have constant comoving number density. Their mass density is then easily obtained as the product of their number density and m_X . Amazingly, if $m_X \approx 300$ GeV, the resulting density of these WIMPs would yield $\Omega_X \sim 0.2 \approx \Omega_{\text{dm}}$, with an uncertainty of about a factor ~ 3 (owing to the as yet unknown detailed properties and thus the precise value of the interaction cross section of X).

Hence, if a massive WIMP exists with properties expected from particle theory—weakly interacting, and with a mass near the weak interaction mass scale—the cosmological density of these particles is just the observed dark matter density! This indeed is an astonishing result, sometimes called the ‘WIMP miracle’, a miracle perhaps too good to be just a random coincidence. For that reason, such a WIMP is the favorite candidate for the dark matter particle. Fortunately, this model can be experimentally verified, and there are three ways how this can be achieved.

Direct detection. The first one is the direct detection. These WIMPs, if they constitute the dark matter in our Galaxy, should also be present in our neighborhood and pass through the Earth. Since they are weakly interacting only, their cross section with ordinary matter is very small, and they are difficult to detect. Nevertheless, experiments were built to search for such particles through their scattering with detector material, i.e., atomic nuclei. Due to scattering, the WIMP will transfer a momentum to the nucleus, and the resulting energy gain can be used for detection. One can estimate the associated recoil energy, given a plausible mass of ~ 300 GeV and the characteristic velocity of ~ 200 km/s,

corresponding to typical velocities in the Galaxy. Then, the kinematics of the scattering process implies that the recoil energy is small, ~ 100 keV. This energy causes a tiny temperature increase of the detector, which must be probed.

Several different methods for the WIMP detection have been turned into experiments. Since WIMP events will be rare, one needs to place the detectors in a well-shielded environment, in laboratories deep underground, so that the background of cosmic ray particles is strongly suppressed. In order to test whether a measured signal is indeed due to particles from outside the Solar system, one checks for an annual variation: Due to the orbit of the Earth around the Sun, our velocity relative to the Galactic frame changes over the year, and the event rate should behave accordingly.

Existing experiments have imposed bounds on combinations of the WIMP mass and its cross section, and ruled out a significant fraction of plausible parameter space. Improvements in the experiments give rise to the expectation that WIMPs can be detected within the next few years. In fact, some experiments have claimed a detection, and also saw an annual modulation. However, the corresponding estimates of the mass and cross section are ruled out by other experiments, so that the interpretation of these results is controversial at present.

Particle colliders. The Large Hadron Collider (LHC) at CERN started operation in 2009; its two major science drivers were the search for the Higgs particle, which has been achieved in the meantime, and the search for phenomena beyond the Standard Model of particle physics. As we argued before, there are good reasons to assume that new physics will appear beyond ~ 100 GeV, an energy range probed by the LHC. However, although the LHC will probably be able to produce WIMPs—if they exist—it will not lead to a direct WIMP detection, due to the low interaction cross sections with matter. Therefore, indirect methods must be used. For example, if supersymmetry is the correct extension of the Standard Model, supersymmetric particles will be produced and decay in the detector, thereby producing the lightest supersymmetric particle—presumably the WIMP. From adding up the charges, momenta and energy of all particles in the reaction, one could then conclude that a neutral particle has left the detector, and get an estimate on its mass. This particle must have a lifetime of $\sim 10^{-7}$ s in order not to decay inside the detector. This lower bound on the lifetime is far away from the requested lifetime $\gg 10^{10}$ yr of the WIMP. Therefore, even though the LHC may point towards the correct physical nature of the WIMP candidate, only its direct detection can prove that it is indeed the dark matter particle. However, from the measured cross sections of other supersymmetric particles, one can determine the free parameters of the model (at least in its simplest version), and

from that get an estimate of the WIMP annihilation cross section. Since this, in combination with the WIMP mass, determines its cosmological density, as explained above, Ω_χ can be estimated in the laboratory! If this value agrees with $\Omega_{\text{dm}} = (\Omega_{\text{m}} - \Omega_{\text{b}})$, then this neutral particle will be indeed an excellent candidate for the dark matter.

Indirect astrophysical detections. In its simplest form, we expect from supersymmetry that the WIMP is its own anti-particle, and thus two WIMPs can annihilate. That happened in the early Universe before the freeze-out of WIMPs, but since then became very rare. Nevertheless, in regions of high dark matter density, some annihilation may occur. The resulting signal depends on the kind of particles into which they annihilate, but in general one would expect that high-energy photons are generated in the decay chain, which may be visible in hard γ -radiation. The number density of annihilation events is proportional to the square of the WIMP density, and therefore the most promising places to look for these γ -rays are probably the centers of dark matter halos—in particular, the center of the Galaxy and that of nearby dwarf galaxies. Of course, the problem of distinguishing the annihilation signal from other γ -ray sources needs to be overcome.

Another indirect method is based on the fact that some WIMPs which cross the Earth or the Sun get scattered by atomic nuclei, thereby change their velocity, which may become lower than the escape velocity from these objects, and thus they are gravitationally captured. After that, they will orbit within the Sun (or the Earth), and due to the high density there, they will scatter again, and finally sink toward the center of the body. Therefore, the density of WIMPs can be strongly enhanced there, and correspondingly the rate of annihilations. The annihilation products will decay, or be stopped, in the body, except for neutrinos which escape. The signature of the annihilation are thus neutrinos, with an energy much higher than produced in nuclear fusion processes. Hence, such high-energy neutrino signals from the center of the Earth or the Sun would be a unique signature of WIMP annihilation. Existing neutrino detectors, such as IceCube in Antarctica, are beginning to probe interesting regions in the WIMP parameter space of mass and cross section.

4.4.7 Recombination

About 3 min after the Big Bang, BBN comes to an end. At this time, the Universe has a temperature of roughly $T \sim 8 \times 10^8$ K and consists of photons, protons, helium nuclei, traces of other light elements, and electrons. In addition, there are neutrinos that dominate, together with photons, the energy density and thus also the expansion rate, and

there are (probably) WIMPs. Except for the neutrinos and the WIMPs, all particle species have the same temperature, which is established by interactions of charged particles with the photons, which resemble some kind of heat bath.

At $z = z_{\text{eq}} \approx 23\,900$ $\Omega_{\text{m}} h^2$, pressureless matter (i.e., the so-called dust) begins to dominate the cosmic energy density and thus the expansion rate. The second term in (4.33) then becomes largest, i.e., $H^2 \approx H_0^2 \Omega_{\text{m}}/a^3$. If a power-law ansatz for the scale factor, $a \propto t^\beta$, is inserted into the expansion equation, we find that $\beta = 2/3$, and hence

$$a(t) = \left(\frac{3}{2} \sqrt{\Omega_{\text{m}}} H_0 t \right)^{2/3} \quad \text{for } a_{\text{eq}} \ll a \ll 1. \quad (4.70)$$

This describes the expansion behavior until either the curvature term or, if this is zero or very small, the Λ -term starts to dominate.

After further cooling, the free electrons can combine with the nuclei and form neutral atoms. This process is called *recombination*, although this expression is misleading: since the Universe was fully ionized until then, it is not a *recombination* but rather the (first) transition to a neutral state—however the expression ‘recombination’ has now long been established. The recombination of electrons and nuclei is in competition with the ionization of neutral atoms by energetic photons (photoionization), whereas collisional ionization can be disregarded completely since η —see (4.65)—is so small. Because photons are so much more numerous than electrons, cooling has to proceed to well below the ionization temperature, corresponding to the binding energy of an electron in hydrogen, before neutral atoms become abundant. This happens for the same reasons as apply in the context of deuterium formation: there are plenty of ionizing photons in the Wien tail of the Planck distribution, even if the temperature is well below the ionization temperature. The ionization energy of hydrogen is $\chi = 13.6\text{ eV}$, corresponding to a temperature of $T > 10^5\text{ K}$, but T has to first decrease to $\sim 3000\text{ K}$ before the ionization fraction

$$x = \frac{\text{number density of free electrons}}{\text{total number density of existing protons}} \quad (4.71)$$

falls considerably below 1, for the reason mentioned above. At temperatures $T > 10^4\text{ K}$ we have $x \approx 1$, i.e., virtually all electrons are free. Only below $z \sim 1300$ does x deviate significantly from unity.

The onset of recombination can be described by an equilibrium consideration which leads to the so-called Saha equation,

$$\frac{1-x}{x^2} \approx 3.84 \eta \left(\frac{k_{\text{B}} T}{m_{\text{e}} c^2} \right)^{3/2} \exp \left(\frac{\chi}{k_{\text{B}} T} \right),$$

which describes the ionization fraction x as a function of temperature. However, once recombination occurs, the assumption of thermodynamical equilibrium is no longer justified. This can be seen as follows:

Any recombination directly to the ground state leads to the emission of a photon with energy $E_\gamma > \chi$. However, these photons can ionize other, already recombined (thus neutral), atoms. Because of the large cross section for photoionization, this happens very efficiently. Thus for each recombination to the ground state, one neutral atom will become ionized, yielding a vanishing net effect. But recombination can also happen in steps, first into an excited state and then evolving into the ground state by radiative transitions. Each of these recombinations will yield a Lyman-series photon in the transition from an excited state into the ground state. This Lyman photon will then immediately excite another atom from the ground state into an excited state, which has an ionization energy of $\leq \chi/4$. This yields no net production of atoms in the ground state. Since the density of photons with $E_\gamma > \chi/4$ is very much larger than of those of $E_\gamma > \chi$, the excited atoms are more easily ionized, and this indeed happens. Stepwise recombination thus also provides no route towards a lower ionization fraction.

The processes described above cause a small distortion of the Planck spectrum due to recombination radiation (in the range $\chi \gg k_{\text{B}} T$) which affects recombination. One cannot get rid of these energetic photons—in contrast to gas nebulae like HII regions, in which the $\text{Ly}\alpha$ photons may escape due to the finite geometry.

Ultimately, recombination takes place by means of a very rare process, the two-photon decay of the first excited level. This process is less probable than the direct $\text{Ly}\alpha$ transition by a factor of $\sim 10^8$. However, it leads to the emission of two photons, neither of which is sufficiently energetic to excite an atom from the ground state. This 2γ -transition is therefore a net sink for energetic photons.¹³ Taking into account all relevant processes and using a rate equation, which describes the evolution of the distribution of particles and photons even in the absence of thermodynamic equilibrium, gives for the ionization fraction in the relevant redshift range $800 \lesssim z \lesssim 1200$

¹³The recombination of hydrogen—and also that of helium which occurred at slightly higher redshifts—perturbed the exact Planck shape of the photon distribution, adding to it the Lyman-alpha photons and the photon pairs from the two-photon transition. This slight perturbation in the CMB spectrum should in principle still be present today. Unfortunately, it lies in a wavelength range ($\sim 200\text{ }\mu\text{m}$) where the dust emission from the Galaxy is very strong; in addition, the wavelength range coincides with the peak of the far-infrared background radiation (see Sect. 9.5.1). Therefore, the detection of this spectral distortion will be extremely difficult.

Fig. 4.18 The first lines of the article by Penzias and Wilson (1965), ApJ 142, 419

A MEASUREMENT OF EXCESS ANTENNA TEMPERATURE AT 4080 Mc/s

Measurements of the effective zenith noise temperature of the 20-foot horn-reflector antenna (Crawford, Hogg, and Hunt 1961) at the Crawford Hill Laboratory, Holmdel, New Jersey, at 4080 Mc/s have yielded a value about 3.5° K higher than expected. This excess temperature is, within the limits of our observations, isotropic, unpolarized, and

$$x(z) = 2.4 \times 10^{-3} \frac{\sqrt{\Omega_m h^2}}{\Omega_b h^2} \left(\frac{z}{1000} \right)^{12.75}. \quad (4.72)$$

The ionization fraction is thus a very strong function of redshift since x changes from 1 (complete ionization) to $x \sim 10^{-4}$ (where essentially all atoms are neutral) within a relatively small redshift range. The recombination process is not complete, however. A small ionization fraction of $x \sim 10^{-4}$ remains since the recombination rate for small x becomes smaller than the expansion rate—some nuclei do not find an electron fast enough before the density of the Universe becomes too low. From (4.72), the optical depth for Thomson scattering (scattering of photons by free electrons) can be computed (see problem 4.12),

$$\tau(z) = 0.37 \left(\frac{z}{1000} \right)^{14.25}, \quad (4.73)$$

which is virtually independent of cosmological parameters. Equation (4.73) implies that photons can propagate from $z \sim 1000$ (the ‘last-scattering surface’) until the present day essentially without any interaction with matter—provided the wavelength is larger than 1216 Å. For photons of smaller wavelength, the absorption cross section of neutral atoms is large. Disregarding these highly energetic photons here—their energies are $\gtrsim 10$ eV, compared to $T_{\text{rec}} \sim 0.3$ eV, so they are far out in the Wien tail of the Planck distribution—we conclude that the photons present after recombination have been able to propagate without further interactions until the present epoch. Before recombination they followed a Planck spectrum. As was discussed in Sect. 4.3.2, the distribution will remain a Planck spectrum with only its temperature changing. Thus these photons from the early Universe should still be observable today, redshifted into the microwave regime of the electromagnetic spectrum.

Our consideration of the early Universe predicts thermal radiation from the Big Bang, as was first realized by George Gamow in 1946—the cosmic microwave background. The CMB is therefore a visible relic of the Big Bang.

The CMB was detected in 1965 by Arno Penzias & Robert Wilson (see Fig. 4.18), who were awarded the 1978 Nobel prize in physics for this very important discovery. At the beginning of the 1990s, the COBE satellite measured the spectrum of the CMB with a very high precision—it is the most perfect blackbody ever measured (see Fig. 4.3). From upper bounds of deviations from the Planck spectrum, very tight limits for possible later energy injections into the photon gas, and thus on energetic processes in the Universe, can be obtained.¹⁴

We have only discussed the recombination of hydrogen. Since helium has a higher ionization energy it recombines earlier than hydrogen. Although recombination defines a rather sharp transition, (4.73) tells us that we receive photons from a recombination layer of finite thickness ($\Delta z \sim 60$). This aspect will be of importance later.

The gas in the intergalactic medium at lower redshift is highly ionized. If this were not the case we would not be able to observe any UV photons from sources at high redshift (‘Gunn-Peterson-test’, see Sect. 8.5.1). Sources with redshifts $z > 6$ have been observed, and we also observe photons with wavelengths shorter than the Ly α line of these objects. Thus at least at the epoch corresponding to redshift $z \sim 6$, the Universe must have been nearly fully ionized or else these photons would have been absorbed by photoionization of neutral hydrogen. This means that at some time between $z \sim 1000$ and $z \sim 6$, a reionization of the intergalactic medium must have occurred, presumably by a first generation of stars or by the first AGNs. The results from the new CMB satellites WMAP and Planck suggest a reionization at redshift $z \sim 10$; this will be discussed more thoroughly in Sect. 8.7.

¹⁴For instance, there exists a cosmic X-ray background (CXB; see Sect. 9.5) which is radiation that appeared isotropic in early measurements. For a long time, a possible explanation for this was suggested to be a hot intergalactic medium with temperature of $k_B T \sim 40$ keV emitting bremsstrahlung radiation. But such a hot intergalactic gas would modify the spectrum of the CMB via the scattering of CMB photons to higher frequencies by energetic electrons (inverse Compton scattering). This explanation for the source of the CXB was excluded by the COBE measurements. From observations by the X-ray satellites ROSAT, Chandra, and XMM-Newton, with their high angular resolution, we know today that the CXB is a superposition of radiation from discrete sources, mostly AGNs.

4.4.8 Summary

We will summarize this somewhat long section as follows:

- Our Universe originated from a very dense, very hot state, the so-called *Big Bang*. Shortly afterwards, it consisted of a mix of various elementary particles, all interacting with each other.
- We are able to examine the history of the Universe in detail, starting at an early epoch where it cooled down by expansion such as to leave only those particle species known to us (electrons, protons, neutrons, neutrinos, and photons), and probably a dark matter particle.
- Because of their weak interaction and the decreasing density, the neutrinos experience only little interaction at temperatures below $\sim 10^{10}$ K, their decoupling temperature.
- At $T \sim 5 \times 10^9$ K, electrons and positrons annihilate into photons. At this low temperature, pair production ceases to take place.
- Protons and neutrons interact and form deuterium nuclei. As soon as $T \sim 10^9$ K, deuterium is no longer efficiently destroyed by energetic photons. Further nuclear reactions produce mainly helium nuclei. About 25 % of the mass in nucleons is transformed into helium, and traces of lithium are produced, but no heavier elements.
- At about $T \sim 3000$ K, some 400 000 years after the Big Bang, the protons and helium nuclei combine with the electrons, and the Universe becomes essentially neutral (we say that it ‘recombines’). From then on, photons can travel without further interactions. At recombination, the photons follow a blackbody distribution (i.e., a thermal spectrum, or a Planck distribution). By the ongoing cosmic expansion, the temperature of the spectral distribution decreases, $T \propto (1 + z)$, though its Planck property remains.
- After recombination, the matter in the Universe is almost completely neutral. However, we know from the observation of sources at very high redshift that the intergalactic medium is essentially fully ionized at $z \lesssim 6$. Before $z > 6$, our Universe must therefore have experienced a phase of reionization. This effect cannot be explained in the context of the *strictly homogeneous* world models; rather it must be examined in the context of structure formation in the Universe and the formation of the first stars and AGNs. These aspects will be discussed in Sect. 10.3.

4.5 Achievements and problems of the standard model

To conclude this chapter, we will evaluate the cosmological model which has been presented. We will review its achievements and successes, but also apparent problems, and

point out the route by which those might be understood. As is always the case in natural sciences, problems with an otherwise very successful model are often the key to a new and deeper understanding.

4.5.1 Achievements

The standard model of the Friedmann–Lemaître universe described above has been extremely successful in numerous ways:

- It predicts that gas which has not been subject to much chemical processing (i.e., metal-poor gas) should have a helium content of ~ 25 %. This is in extraordinarily good agreement with observations.
- It predicts that sources of lower redshift are closer to us than sources of higher redshift.¹⁵ Therefore, modulo any peculiar velocities, the absorption of radiation from sources at high redshift must happen at smaller redshifts. Not a single counter-example has been found yet.
- It predicts the existence of a microwave background, which indeed was found.
- It predicts the correct number of neutrino families, which was confirmed in laboratory experiments of the Z-boson decay.

Further achievements will be discussed in the context of structure evolution in the Universe.

A good physical model is one that can also be falsified. In this respect, the Friedmann–Lemaître universe is also an excellent model: a single observation could either cause a lot of trouble for this model or even disprove it. To wit, it would be incompatible with the model

1. if the helium content of a gas cloud or of a low-metallicity star was significantly below 25 %;
2. if it was found that one of the neutrinos has a rest mass $\gtrsim 100$ eV;
3. if the Wien-part of the CMB had a smaller amplitude compared to the Planck spectrum;
4. if a source with emission lines at z_e was found to show absorption lines at $z_a \gg z_e$;
5. if the cosmological parameters were such that $t_0 \lesssim 10$ Gyr.

On (1): While the helium content may increase by stellar evolution due to fusion of hydrogen into helium, only a small fraction of helium is burned in stars. In this process, heavier elements are of course produced. A gas cloud or a star with low metallicity therefore cannot consist of material in which helium has been destroyed; it must contain at least the helium abundance from BBN. On (2): Such a

¹⁵We ignore peculiar motions here which may cause an additional (Doppler-)redshift. These are typically $\lesssim 1000$ km/s and are thus small compared to cosmological redshifts.

neutrino would lead to $\Omega_m > 2$, which is in strict contradiction to the derived model parameters. On (3): Though it is possible to generate additional photons by energetic processes in the past, thereby increasing the Wien-part of the coadded spectrum compared to that of a Planck function, it is thermodynamically impossible to extract photons from the Wien-part. On (4): Such an observation would question the role of redshift as a monotonic measure of relative distances and thus remove one of the pillars of the model. On (5): Our knowledge of stellar evolution allows us to determine the age of the oldest stars with a precision of better than $\sim 20\%$. An age of the Universe below ~ 10 Gyr would be incompatible with the age of the globular clusters—naturally, these have to be younger than the age of our Universe, i.e., the time after the Big Bang.

Although these predictions have been known for more than 40 years, no observation has yet been made which disproves the standard model. Indeed, at any given time there have been astronomers who like to disagree with the standard model. These astronomers have tried to make a discovery, like the examples above, which would pose great difficulties for the model. So far without success; this does not mean that such results cannot be found in the literature, but rather such results did not withstand closer examination. The simple opportunities to falsify the model and the lack of any corresponding observation, together with the achievements listed above, have made the Friedmann–Lemaître model *the* standard model of cosmology. Alternative models have either been excluded by observation (such as steady-state cosmology) or have been unable to make any predictions. Currently, there is no serious alternative to the standard model.

4.5.2 Problems of the standard model

Despite these achievements, there are some aspects of the model which require further consideration. Here we will describe two conceptual problems with the standard model more thoroughly—the horizon problem and the flatness problem.

Horizons. The finite speed of light implies that we are only able to observe a finite part of the Universe, namely those regions from which light can reach us within a time t_0 . Since $t_0 \approx 13.8$ Gyr, our visible Universe has—roughly speaking—a radius of 13.8 billion light years. More distant parts of the Universe are at the present time unobservable for us. This means that there exists a horizon beyond which we cannot see. Such horizons do not only exist for us today: at an earlier time t , the size of the horizon was about ct , hence smaller than today. We will now describe this aspect quantitatively.

In a time interval dt , light travels a distance $c dt$, which corresponds to a comoving distance interval $dx = c dt/a$ at scale factor a . From the Big Bang to a time t (or redshift z) the light traverses a comoving distance of

$$r_{\text{H,com}}(z) = \int_0^t \frac{c dt}{a(t)}.$$

From $\dot{a} = da/dt$ we get $dt = da/\dot{a} = da/(aH)$, so that

$$r_{\text{H,com}}(z) = \int_0^{(1+z)^{-1}} \frac{c da}{a^2 H(a)}. \quad (4.74)$$

If $z_{\text{eq}} \gg z \gg 0$, the main contribution to the integral comes from times (or values of a) in which pressureless matter dominates the expansion rate H . Then with (4.33) we find $H(a) \approx H_0 \sqrt{\Omega_m} a^{-3/2}$, and (4.74) yields

$$r_{\text{H,com}}(z) \approx 2 \frac{c}{H_0} \frac{1}{\sqrt{(1+z)\Omega_m}} \quad \text{for } z_{\text{eq}} \gg z \gg 0. \quad (4.75)$$

In earlier phases, $z \gg z_{\text{eq}}$, H is radiation-dominated, $H(a) \approx H_0 \sqrt{\Omega_r}/a^2$, and (4.74) becomes

$$r_{\text{H,com}}(z) \approx \frac{c}{H_0 \sqrt{\Omega_r}} \frac{1}{(1+z)} \quad \text{for } z \gg z_{\text{eq}}. \quad (4.76)$$

The earlier the cosmic epoch, the smaller the comoving horizon length, as was to be expected. In particular, we will now consider the recombination epoch, $z_{\text{rec}} \sim 1000$, for which (4.75) applies (see Fig. 4.19). The comoving length $r_{\text{H,com}}$ corresponds to a physical proper length $r_{\text{H,prop}} = a r_{\text{H,com}}$, and thus

$$r_{\text{H,prop}}(z_{\text{rec}}) = 2 \frac{c}{H_0} \Omega_m^{-1/2} (1 + z_{\text{rec}})^{-3/2} \quad (4.77)$$

is the horizon length at recombination. We can then calculate the angular size on the sky that this length corresponds to,

$$\theta_{\text{H,rec}} = \frac{r_{\text{H,prop}}(z_{\text{rec}})}{D_A(z_{\text{rec}})},$$

where D_A is the angular-diameter distance (4.49) to the last scattering surface of the CMB. Using (4.51), we find that in the case of $\Omega_A = 0$

$$D_A(z) \approx \frac{c}{H_0} \frac{2}{\Omega_m z} \quad \text{for } z \gg 1,$$

and hence

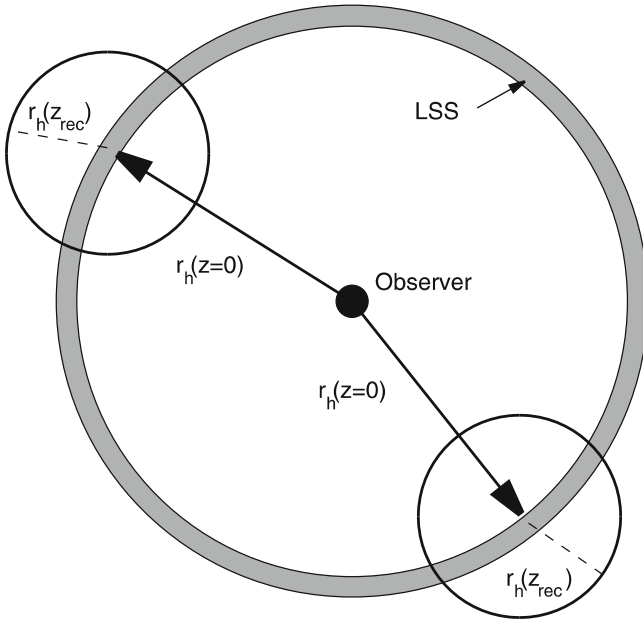


Fig. 4.19 The horizon problem: the region of space which was in causal contact before recombination has a much smaller radius than the spatial separation between two regions from which we receive the CMB photons. Thus the question arises how these two regions may ‘know’ of each other’s temperature. Adapted from: Alan Guth 1998, *The inflationary Universe*, Basic Books

$$\theta_{\text{H,rec}} \approx \sqrt{\frac{\Omega_m}{z_{\text{rec}}}} \sim \frac{\sqrt{\Omega_m}}{30} \sim \sqrt{\Omega_m} 2^\circ \text{ for } \Omega_\Lambda = 0. \quad (4.78)$$

This means that the horizon length at recombination subtends an angle of about 1° on the sky.

The horizon problem: Since no signal can travel faster than light, (4.78) means that CMB radiation from two directions separated by more than about one degree originates in regions that were not in causal contact before recombination, i.e., the time when the CMB photons interacted with matter the last time. Therefore, these two regions have never been able to exchange information, for example about their temperature. Nevertheless their temperature is the same, as seen from the high degree of isotropy of the CMB, which shows relative fluctuations of only $\Delta T/T \sim 10^{-5}$!

Redshift-dependent density parameter. We have defined the density parameters Ω_m and Ω_Λ as the current density divided by the critical mass density ρ_{cr} today. These definitions can be generalized. If we existed at a different time, the densities and the Hubble constant would have had different

values and consequently we would obtain different values for the density parameters. Thus we define the total density parameter for an arbitrary redshift

$$\Omega_0(z) = \frac{\rho_m(z) + \rho_r(z) + \rho_v}{\rho_{\text{cr}}(z)}, \quad (4.79)$$

where the critical density ρ_{cr} is also a function of redshift,

$$\rho_{\text{cr}}(z) = \frac{3H^2(z)}{8\pi G}. \quad (4.80)$$

Then by inserting (4.24) into (4.79), we find

$$\Omega_0(z) = \left(\frac{H_0}{H}\right)^2 \left(\frac{\Omega_m}{a^3} + \frac{\Omega_r}{a^4} + \Omega_\Lambda\right).$$

Using (4.33), this yields

$$1 - \Omega_0(z) = F [1 - \Omega_0(0)], \quad (4.81)$$

where $\Omega_0(0)$ is the total density parameter today, and

$$F = \left(\frac{H_0}{a H(a)}\right)^2. \quad (4.82)$$

From (4.81) we can now draw two important conclusions. Since $F > 0$ for all a , the sign of $(\Omega_0 - 1)$ is preserved and thus is the same at all times as today. Since the sign of $(\Omega_0 - 1)$ is the same as that of the curvature—see (4.32)—the sign of the curvature is preserved in cosmic evolution: a flat Universe will be flat at all times, a closed Universe with $K > 0$ will always have a positive curvature.

The second conclusion follows from the analysis of the function F at early cosmic epochs, e.g., at $z \gg z_{\text{eq}}$, thus in the radiation-dominated Universe. Back then, with (4.33), we have

$$F = \frac{1}{\Omega_r(1+z)^2},$$

so that for very early times, F becomes very small. For instance, at $z \sim 10^{10}$, the epoch of neutrino freeze-out, $F \sim 10^{-15}$. Today, Ω_0 is of order unity; from observations, we know that certainly $0.1 \lesssim \Omega_0(0) \lesssim 2$, where this is a *very* generous estimate,¹⁶ so that $|1 - \Omega_0(0)| \lesssim 1$. Since F is so small at large redshifts, this means that $\Omega_0(z)$ must have been

¹⁶From the most recent CMB measurements (see Sect. 8.7) we are able to constrain this interval to better than $[0.99, 1.01]$.

very, very close to 1; for example at $z \sim 10^{10}$ it is required that $|\Omega_0 - 1| \lesssim 10^{-15}$.

Flatness problem: For the total density parameter to be of order unity today, it must have been extremely close to 1 at earlier times, which means that a very precise ‘fine tuning’ of this parameter was necessary.

This aspect can be illustrated very well by another physical example. If we throw an object up into the air, it takes several seconds until it falls back to the ground. The higher the initial velocity, the longer it takes to hit the ground. To increase the time of flight we need to increase the initial velocity, for instance by using a cannon. In this way, the time of flight may be extended to up to about a minute. Assume that we want the object to be back only after one day; in this case we must use a rocket. But we know that if the initial velocity of a rocket exceeds the escape velocity $v_{\text{esc}} \sim 11.2 \text{ km/s}$, it will leave the gravitational field of the Earth and never fall back. On the other hand, if the initial velocity is too much below v_{esc} , the object will be back in significantly less than a day. So the initial velocity must be *very* well chosen for the object to return after being up for at least a day. The flatness problem is completely analogous to this.

Let us consider the consequences of the case where Ω_0 had not been so extremely close to 1 at $z \sim 10^{10}$; then, the universe would have recollapsed long ago, or it would have expanded significantly faster than the universe we live in. In either case, the consequences for the evolution of life in the universe would have been catastrophic. In the first case, the total lifetime of the universe would have been much shorter than is needed for the formation of the first stars and the first planetary systems, so that in such a world no life could be formed. In the second case, extreme expansion would have prevented the formation of structure in the universe. In such a universe no life could have evolved either.

This consideration can be interpreted as follows: we live in a universe which had, at a very early time, a very precisely tuned density parameter, because only in such a universe can life evolve and astronomers exist to examine the flatness of the universe. In all other conceivable universes this would not be possible. This approach is meaningful only if a large number of universes existed—in this case we should not be too surprised about living in one of those where this initial fine-tuning took place—in the other ones, we, and the question about the cosmological parameters, would just not exist. This approach is called the *anthropic principle*. It may either be seen as an ‘explanation’ for the flatness of *our* Universe, or as a capitulation—where we give up to explore a physical reason for the origin of the flatness of our Universe.

The example of the rocket given above is helpful in understanding another aspect of cosmic expansion. If the

rocket is supposed to have a long time of flight but not escape the gravitational field of the Earth, its initial velocity must be very, very close to, but a tiny little bit smaller than v_{esc} . In other words, the absolute value of the sum of kinetic and potential energy has to be very much smaller than either of these two components. This is also true for a large part of the initial trajectory. Independent of the exact value of the time of flight, the initial trajectory can be approximated by the limiting case $v_0 = v_{\text{esc}}$ at which the total energy is exactly zero. Transferred to the Hubble expansion, this reads as follows: independent of the exact values of the cosmological parameters, the curvature term can be disregarded in the early phases of expansion (as we have already seen above). This is because our Universe can reach its current age only if at early times the modulus of potential and kinetic energy were nearly exactly equal, i.e., the curvature term in (4.14) must have been a lot smaller than the other two terms.

4.5.3 Extension of the standard model: inflation

We will consider the horizon and flatness problems from a different, more technical point of view. Einstein’s field equations of GR, one solution of which has been described as our world model, are a system of coupled partial differential equations. As is always the case for differential equations, their solutions are determined by (1) the system of equations itself and (2) the initial conditions. If the initial conditions at, e.g., $t = 1 \text{ s}$ were as they have been described, the two aforementioned problems would not exist. But why are the conditions at $t = 1 \text{ s}$ such that they lead to a homogeneous, isotropic, (nearly) flat model? The set of homogeneous and isotropic solutions to the Einstein equation is of measure zero (i.e., nearly all solutions of the Einstein equation are not homogeneous and isotropic); thus these particular solutions are *very* special. Taking the line of reasoning that the initial conditions ‘just happened to be so’ is not satisfying because it does not explain anything. Besides the anthropic principle, the answer to this question can only be that processes must have taken place even earlier, due to known or as yet unknown physics, which have produced these ‘initial conditions’ at $t = 1 \text{ s}$. The initial conditions of the normal Friedmann–Lemaître expansion thus have a physical origin. Cosmologists believe they have found such a physical reason: the inflationary model.

Inflation. In the early 1980s, a model was developed which was able to solve the flatness and horizon problems (and some others as well). As a motivation for this model, we first recall that the physical laws and properties of elementary particles are well known up to energies of $\sim 100 \text{ GeV}$ because they were experimentally tested in particle accelerators. For

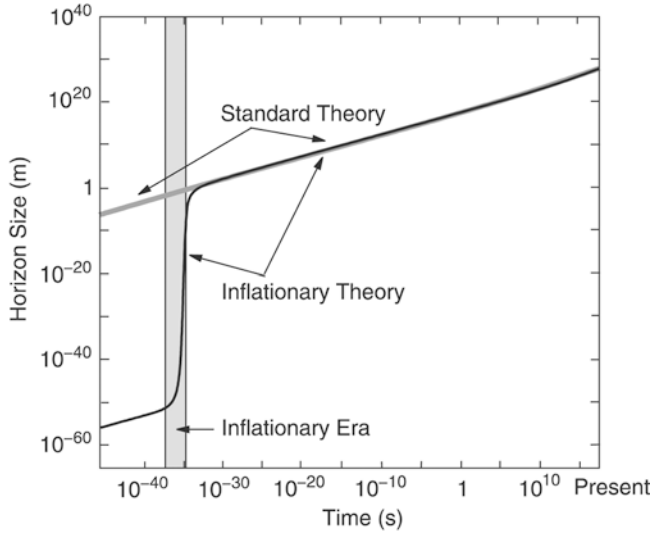


Fig. 4.20 During an inflationary phase, indicated here by the gray bar, the universe expands exponentially; see (4.83). This phase comes to an end when a phase transition transforms the vacuum energy into matter and radiation, after which the universe follows the normal Friedmann expansion. Adapted from: Alan Guth 1998, *The inflationary Universe*, Basic Books

higher energies, particles and their interactions are unknown. This means that the history of the Universe, as sketched above, can be considered secure only up to energies of 100 GeV. The extrapolation to earlier times, up to the Big Bang, is considerably less certain. From particle physics we expect new phenomena to occur at an energy scale of the Grand Unified Theories (GUTs), at about 10^{14} GeV, corresponding to $t \sim 10^{-34}$ s.

In the inflationary scenario it is presumed that at very early times the vacuum energy density was much higher than today, so that it dominated the Hubble expansion. Then from (4.18) we find that $\dot{a}/a \approx \sqrt{\Lambda/3}$. This implies an exponential expansion of the Universe,

$$a(t) = C \exp\left(\sqrt{\frac{\Lambda}{3}} t\right). \quad (4.83)$$

Obviously, this exponential expansion (or inflationary phase) cannot last forever. We assume that a phase transition took place in which the vacuum energy density is transformed into normal matter and radiation (a process called reheating), which ends the exponential expansion and after which the normal Friedmann evolution of the Universe begins. Figure 4.20 sketches the expansion history of the universe in an inflationary model.

Inflation solves the horizon problem. During inflation, $H(a) = \sqrt{\Lambda/3}$ is constant so that the integral (4.74) for the comoving horizon length formally diverges. This implies that the horizon may become arbitrarily large in the infla-

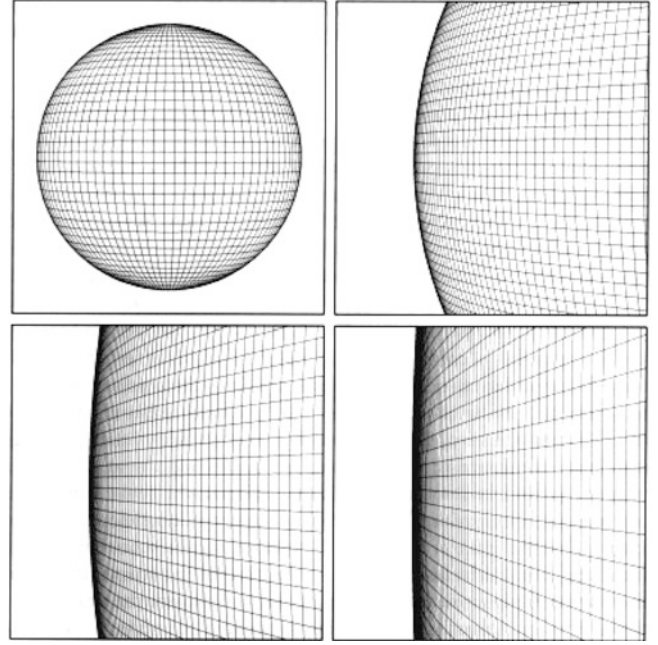


Fig. 4.21 Due to tremendous expansion during inflation, even a universe with initial curvature will appear to be a flat universe by the end of the inflationary phase. Source: A.H. Guth 1998, *The Inflationary Universe*, Basic Books

tionary phase, depending on the duration of the exponential expansion. For illustration we consider a very small region in space of size $L < ct_i$ at a time $t_i \sim 10^{-34}$ s prior to inflation which is in causal contact. Through inflation, it expands tremendously, e.g., by a factor $\sim 10^{40}$; the original $L \sim 10^{-24}$ cm inflate to about 10^{16} cm by the end of the inflationary phase, at $t_f \sim 10^{-32}$ s. By today, this spatial region will have expanded by another factor of $\sim 10^{25}$ by following (for $t > t_f$) the normal cosmic expansion, to $\sim 10^{41}$ cm. This scale is considerably larger than the size of the currently visible Universe, c/H_0 . According to this scenario, the whole Universe visible today was in causal contact prior to inflation, so that the homogeneity of the physical conditions at recombination, and with it the nearly perfect isotropy of the CMB, is provided by causal processes.

Inflation solves the flatness problem as well. Due to the tremendous expansion, any initial curvature is straightened out (see Fig. 4.21). Formally this can be seen as follows: during the inflationary phase we have

$$\Omega_\Lambda = \frac{\Lambda}{3H^2} = 1,$$

and since it is assumed that the inflationary phase lasts long enough for the vacuum energy to be completely dominant, when it ends we then have $\Omega_0 = 1$. Hence the universe is flat to an extremely good approximation.

The inflationary model of the very early universe predicts that today $\Omega_0 = 1$ is valid to very high precision; any other value of Ω_0 would require another fine-tuning. Thus our Universe is expected to be flat.

The physical details of the inflationary scenario are not very well known. In particular it is not yet understood how the phase transition at the end of the inflationary phase took place and why it did not occur earlier. But the two achievements presented above (and some others) make an inflationary phase appear a very plausible scenario. As we will see below (Chap. 8), the prediction of a flat universe was recently accurately tested and it was indeed confirmed. Furthermore, the inflationary model provides a natural, and in fact the only plausible, explanation for the origin of density fluctuations in the Universe which must have been present at very early epochs as the seeds of structure formation. We will discuss these aspects further in Chap. 7.

4.6 Problems

4.1. Big Bang Nucleosynthesis.

1. Calculate the baryon density at the epoch of nucleosynthesis. How does it compare with the density in the central regions of stars where nuclear burning takes place?
2. It takes the Sun some ten billion years to convert $\sim 10\%$ of its hydrogen into helium, whereas in BBN, all helium is formed on a time-scale of a minute. Can you speculate about the reasons for this difference?
3. During BBN, energy is released from the fusion process. Obtain an estimate of this fusion energy generated per unit volume, and compare it to the energy density of the photons at the epoch of BBN. Does BBN cause a substantial heating of the Universe?

4.2. Deceleration parameter. Assume that the energy density of the universe is composed of N different species. Each of these species is characterized by a density parameter Ω_i and an equation-of-state parameter w_i which describes the relation between pressure and density, $P_i = w_i \rho_i c^2$. Calculate the deceleration parameter q_0 for this cosmological model. By specializing to the three energy components discussed in this chapter, can you rederive (4.35)?

4.3. The qualitative behavior of the cosmic expansion.

The general discussion of the qualitative behavior of the solutions of the Friedmann equation (4.33) is tedious, but some special results can be derived quite easily. In the following, neglect the (very small) contribution from Ω_r .

1. For $\Omega_\Lambda = 0$, show that the universe has been expanding for all $0 < a \leq 1$, that it will continue to expand forever in the future if $\Omega_m \leq 1$, and that it reaches a maximum expansion at t_{\max} , corresponding to the maximum scale factor a_{\max} . Calculate a_{\max} as a function of Ω_m .
2. Show that the universe expands forever in the future if $\Omega_\Lambda \geq 0$ and $\Omega_m \leq 1$, and that it has been expanding in the past if $0 \leq \Omega_\Lambda < 1$, irrespective of Ω_m .
3. For the case of a closed universe which has a maximum expansion factor, or that of a bouncing model where a minimum scale factor occurs, show that $a(t_{\text{ex}} - t) = a(t_{\text{ex}} + t)$, where t_{ex} is the time where the extremum of the scale factor is attained.

4.4. Expansion law in a flat universe. You will now solve the Friedmann equation (4.33) for the case of vanishing curvature and vanishing radiation density. This describes the model of the Universe we live in, for scale factors $a \gg a_{\text{eq}}$.

1. As a first step, write $a = v^\beta$, and choose β such that the Friedmann equation can be brought to the form $\dot{v}^2 = A + Bv^2$.
2. Then make the ansatz $v(t) = v_0 \sinh(t/t_a)$, and determine v_0 and t_a such that the foregoing equation is solved. Note that $\sinh'(x) = \cosh(x)$ and $\cosh^2(x) = 1 + \sinh^2(x)$.
3. Combining these two steps, write the full solution $a(t)$ explicitly. What is the behavior of the solution for $t \ll t_a$ and for $t \gg t_a$ —does it agree with your expectations? Does this solution describe the transition from a decelerating expansion to an accelerated one?

4.5. The onset of inflation. Solve the Friedmann equation for a flat universe with vanishing matter density—the situation perhaps approximating the situation in our Universe before the end of inflation. Use the same steps as in the previous problem to obtain the solution. Again, there is a characteristic time scale t_a occurring in the solution; what is the behavior of the scale factor for $t \ll t_a$ and for $t \gg t_a$? Does this correspond to what is written in the main text for radiation dominance and vacuum energy dominance, respectively?

4.6. Distances in cosmology. In Sect. 4.3.3, we quoted the expressions for the angular-diameter distance as a function of redshift; these expressions shall be derived here.

1. Consider a radial light ray reaching us today, i.e., at scale factor $a = 1$. From the relation (4.39), derive the relation between a small interval da and a comoving radial distance interval dx along this ray.
2. Using this result, show that the comoving distance as a function of redshift is given by (4.53).
3. For a flat universe with $K = 0$, show the angular-diameter distance is given by (4.54).

4.7. Expansion law in an $\Omega_\Lambda = 0$ universe. For a model with vanishing vacuum density, the expansion law can be obtained analytically.

1. As preparation for the solution, we consider a differential equation of the form

$$\left(\frac{df}{dt}\right)^2 = \frac{C}{f} - K, \quad (4.84)$$

where $C > 0$ and K are constants. Solutions of (4.84) are given in parametric form. Show by insertion that the solution with $f(t_1) = 0$ reads

$$f(\theta) = \frac{C}{2K} (1 - \cos \theta), \quad t(\theta) = t_1 + \frac{C}{2K^{3/2}} (\theta - \sin \theta) \quad (4.85)$$

for $K > 0$ and $0 \leq \theta \leq 2\pi$, and

$$f(\theta) = \frac{C}{2|K|} (\cosh \theta - 1), \quad t(\theta) = t_1 + \frac{C}{2|K|^{3/2}} (\sinh \theta - \theta) \quad (4.86)$$

for $K < 0$ and $\theta \geq 0$. Note that $df/dt = (df/d\theta)(dt/d\theta)^{-1}$. In the special case of $K = 0$, show that the solution is

$$f(t) = \left(\frac{9C}{4}\right)^{1/3} (t - t_1)^{2/3}. \quad (4.87)$$

For the case of $K > 0$, show that f reaches a maximum value $f_{\max} = C/K$ at time $t_{\max} = t_1 + \pi CK^{-3/2}/2$, and that $f_{\text{coll}} = 0$ at time $t_{\text{coll}} = t_1 + \pi CK^{-3/2}$.

2. Show that the Friedmann equation (4.33) in the case of $\Omega_\Lambda = 0 = \Omega_r$ is of the form (4.84), and derive the expansion law in parametric form. Does the maximum scale factor a_{\max} that occurs for $\Omega_m > 1$ agree with what you found in problem 4.3? At what cosmic time does this maximum scale factor occur? When does such a universe recollapse?
3. As in problem 1.4, consider a sphere of mass M and initial radius r_0 at time $t = 0$, collapsing due to gravity. Show that the equation of motion for $r(t)$ can be written in the form (4.84), and determine the physical meaning of C and K . Show that the solution derived in problem 1.4 corresponds to the case $K = 0$. If the sphere at $t = 0$ was at rest, $\dot{r}(0) = 0$, show that the sphere collapses to point within the *free-fall time*

$$t_{\text{ff}} = \sqrt{\frac{3\pi}{32G\bar{\rho}}}, \quad (4.88)$$

where $\bar{\rho}$ is the initial mean density of the sphere.

4.8. The time of return for a upward-moving object. In the text, an analogon of a nearly flat universe has been given, namely that of an object shot vertically upwards from the surface of the Earth. The time at which it returns to the surface is either ‘short’, or the velocity has to be very well fine-tuned. Using the parametric solution of the equation of motion derived in the previous exercise, we can now consider this situation quantitatively.

1. Show that the equation of motion for the object can be written in the form $\dot{r}^2 = 2GM_E/r - K$, where M_E is the mass of the Earth. Relate the integration constant K to the initial velocity v_0 of the object, and assume in the following that $v_0 < v_{\text{esc}}$, where $v_{\text{esc}} = \sqrt{2GM_E/r_E} \approx 11.2$ km/s, with $r_E \approx 6380$ km being the Earth’s radius.
2. From the parametric solution of the last problem, calculate the time t_{ret} at which the object returns to the Earth surface. For this, you can assume that the time-of-flight is ‘long’, i.e., much longer than r_E/v_0 . Then find the relation between K and the time t_{ret} .
3. Combining the last two steps, obtain the relation between the initial velocity v_0 and the time of return t_{ret} . What fraction of the escape velocity does the object have to have initially if it should return after 1 day (1 year)?

4.9. Baryon cooling in the Universe. Suppose that at some epoch after recombination, the baryons are fully decoupled from the photons, so that there is no energy transfer from one species to the other. Use (4.47) to derive the expected redshift dependence of the baryon temperature during this epoch.

4.10. Thermal velocity of the cosmic neutrino background. Using (4.47), calculate the current characteristic velocity of neutrinos that decoupled in the early phase of the Big Bang.

4.11. Some properties of the Einstein–de Sitter model. Consider the Einstein–de Sitter model.

1. Calculate the look-back time $\tau(z)$. At what redshift was the age of the Universe half of its current age?
2. What is the volume of the spherical shell between redshifts z and $z + \Delta z$?
3. Assume the comoving density n_{com} of a class of cosmic objects is constant; how many of these are contained in sphere around us with maximum redshift z ? Check that your result agrees with the expected one for $z \ll 1$.

4.12. The dependence of BBN on $\Omega_b h^2$. The expansion law (4.61) yields the cosmic time vs. temperature. Why does this relation not depend on the Hubble constant? Why does the helium yield Y depend on the combination $\Omega_b h^2$ —see (4.68)—and not just on Ω_b ?

4.13. Recombination optical depth. Using (4.72), show that the optical depth to Thomson scattering is almost independent of the cosmological parameters, as given in (4.73).

Extragalactic Astronomy and Cosmology

An Introduction

Schneider, P.

2015, XVIII, 626 p. 514 illus., 323 illus. in color.,

Hardcover

ISBN: 978-3-642-54082-0